B-1 derived anti-Thy-1 B cells in old aged mice develop lymphoma/leukemia with high expression of CD11b and Hamp2 that different from TCL1 transgenic mice

Kyoko Hayakawa[1*], Yan Zhou[1] and Susan A. Shinton[1]

Abstract

Human old aged unmutated chronic lymphocytic leukemia U-CLL are the TCL1$^+$ZAP70$^+$CD5$^+$ B cells. Since CD5 makes the BCR signaling tolerance, ZAP70 increased in U-CLL not only TCL1$^+$ alone. In mice, TCL1 (TCL1A) is the negative from neonate to old aged, as TC$^-$. V$_H$8-12/V$_k$21-5 is the anti-thymocyte/Thy-1 autoreactive ATA B cell. When ATA µκTg generation in mice, ATA B cells are the neonate generated CD5$^+$ B cells in B-1, and in the middle age, CD5$^+$ can be down or continuously CD5$^+$, then, old aged CLL/lymphoma generation with increased CD11b in TC$^-$ZAP70$^-$CD5$^-$ or TC$^-$ZAP70$^+$CD5$^+$. In this old aged TC$^-$ATA B microarray analysis showed most similar to human CLL and U-CLL, and TC$^-$ZAP70$^+$CD5$^+$ showed certain higher present as U-CLL. Original neonate ATA B cells showed with several genes down or further increase in old aged tumor, and old aged T-bet$^+$CD11c$^+$, CTNNB1^{hi}, HMGB^{hi}, CXCR4^{hi}, DPP4^{hi} and decreased miR181b. These old aged increased genes and down miR181b are similar to human CLL. Also, in old age ATA B cell tumor, high CD38^{++}CD44^{++}, increased Ki67$^+$ AID$^+$, and decreased CD180$^-$ miR15O^{low} are similar to U-CLL. In this old aged ATA B, increased TLR7,9 and Wnt10b. TC$^+$Tg generated with ATAµκTg mice occurred middle age tumor as TC$^+$ZAP70$^-$CD5$^+$ or TC$^+$ZAP70$^+$CD5$^+$, with high NF-kB1, TLR4,6 and Wnt5b,6 without increased CD11b. Since neonatal state to age with TC$^+$Tg continuously, middle age CLL/lymphoma generation is not similar to old aged generated, however, some increased in TC$^+$ZAP70$^+$ are similar to the old age TC$^-$ ATA B tumor. Then, TC$^-$ ATA B old age tumor showed some difference to human CLL. ATA B cells showed CD11b$^+$CD22^{++}, CD24 down, and hepcidin Hamp2^{++} with iron down. This mouse V8-12 similar to human V2-5, and V2-5 showed several cancers with macrophages/neutrophils generated hepcidin$^+$ iron^{low} or some showed hepcidin$^-$ iron$^+$ with tumor, and mouse V8-12 with different V$_k$19-17 generate MZ B cells strongly increased macrophage^{++} in old aged and generated intestine/colon tumor. Conclusion, neonate generated TC$^-$ATA B1 cells in old aged tumor generation are CD11b$^+$ in the leukemia CLL together with lymphoma cancer with hepcidin-related Hamp2^{++} in B-1 cell generation to control iron.

Keywords B1, CLL/lymphoma, TC$^+$ Tg, CD11b, Hamp2, V2-5

Introduction

In human and mice, the Lin28b$^+$Let7$^-$ axis plays a major role in fetal/neonatal development, whereas Lin28$^-$Let7$^+$ cells are more important in adults [1]. In old age, function of the adaptive immune system is diminished [2], whereas increased function of the innate immune system is more important such as myeloid cell differentiation

*Correspondence:
Kyoko Hayakawa
Kyoko.Hayakawa@me.com
[1] Fox Chase Cancer Center, 333 Cottman Ave., Philadelphia, PA 19111, USA

Hayakawa *et al. Immunity & Ageing*   (2024) 21:22

Page 2 of 24

and fetal/neonatal origin B-1 B cells. In old age in human, chronic lymphocyte leukemia (CLL) is the most common type of leukemia in Western countries. Human CLL is CD5^{+} B cells and is often found with mutated IGH gene (M-CLL) which has a significantly better overall survival than patients with unmutated (U-CLL) [3, 4]. U-CLL often found as IGHV1-69, which can originate in the fetal/neonatal stage from cord blood [5]. Overall, CLL is lower in Africa than in Western countries, however CLL originating in Africa showed higher incidence of U-CLL with V1-69 than M-CLL [6]. Since original fetal/neonate generation levels and adult B and T cell interaction with containing original B-1 cells, early origin background is important to old age in U-CLL.

In mice, CLL is rarely observed. However, NZB mice show CLL generation [7] and NZB cells showed high NTA(natural thymocytotoxic autoantibodies) expression associated with CD5^{+} B cells [8]. Most mice generate NTA expression, and SM/J and NZB mice express higher NTA than BALB/c and C57BL/6 [9]. We first found NTA expression in SM/J mice at the immature T cell stage drives positive selection of B cells with high expression of V_H8-12/V_k21-5 BCR, which showed anti-thymocyte/Thy-1 autoreactive (ATA) B cells [10]. We then, generated ATAμκTg in C.B17 mice (BALB/c–Igh[b]), in which ATA B (Igh[a]) cells are the largely product of fetal/neonatal B cell development (B-1) as CD5^{+}B1a, normally constituting B-1 cell subset in adult, as B1 B cells [11]. In adult B cell development (B-2) from BM, the expression of V_H8-12/V_k21-5 BCR drives negative selection, resulting in developmental arrest [11]. Then, these B-1 origin V_H8-12/V_k21-5 ATA B cells can generate leukemia/lymphoma in old aged with increased expression of CD11b [12, 13]. This paper now showed with CD11b-CD22^{++}, and also found that very high level of hepcidin-Hamp2 in ATA B cells in old age.

Mouse ATA B leukemia/lymphoma are TC^{−}, α-Thy-1 ATA B cell, and Hamp2^{++}. These differences between human versus mice. In human CLL, TCL1^{+} positive and U-CLL CD5^{+} B cells with ZAP70^{+}. TCL1 (TCL1A,B) are expressed in the embryonic stage in mice and human, originally [14, 15]. Then, in mice, TCL1 (TCL1A) is down regulated in fetal liver and then negative in neonate, becoming TCL1^{−} through adulthood [16]. In human, Pro-B, Pre-B, and immature B cells are TCL1^{+}, and in spleen, TCL1 is still positive in immature B cells, then decreased in mature B cells to minimal levels [17]. Then, vascuration made to increase TCL1 in human cells and original B-1 unmutated CD5^{+} B cells can increased with TC^{+} [18, 19], also adult B cells can generated mutated CD5^{+} B cells with TC^{+}. CD5 binds to SHR-1 related to the BCR, CD5 makes the BCR signaling tolerance [20, 21]. Thus, not only TCL1^{+} which BCR signaling hyperresponsive

[22], ZAP70^{+} made more responses in human U-CLL for further response with autoimmune predisposition, showed TC^{+}ZAP70^{+}CD5^{+} [23]. In aged mice, B cells are continuously TCL1^{−} (TC^{−}). Some original TC^{−} CD5^{+} B1a cells can downregulate CD5 in aged [24, 25]. Thus, ATAμκTg B lymphoma/leukemia can be generated from TC^{−}ZAP70^{−}CD5^{−}, or TC^{−}ZAP70^{+}CD5[+](or CD5^{−}) B1 cells. We previously observed that transgenic expression of TCL1[+](TC^{+})Tg in ATA B cells induced CLL/leukemia in middle aged mice [24], which originated from TC^{+}ZAP70^{−}CD5^{+} or TC^{+}ZAP70^{+}CD5[+](or CD5^{−}) B1 cells. Since human U-CLL is TC^{+}ZAP70^{+}CD5^{+}, we further compared TC^{−} and TC^{+}Tg ATAμκTg mice by microarray analysis, to determine why TC^{+}Tg mice showed lymphoma/leukemia development in middle age instead of old aged. In this paper, we found that RagKO ThyKO ATAμκTg mice which were TC^{−}CD5^{−}Thy-1^{−} and lacked mature T and B cells, showed high ZAP70^{+} B1 cells with early state of CLL/lymphoma. In addition to being ZAP70^{+}, we found old aged generated ATA B TC^{−}ZAP70^{−}CD5^{−} B1 cells with CD11b^{++}, most of which were similar to old aged human TC^{+}CLL/U-CLL cells.

Thy-1(CD90) is heavily N-glycosylated, glycophosphatidylinositol anchored cell surface protein. Thy-1 controls inflammatory cell recruitment in human and mice [26, 27], and Thy-1 plays an important role in the initial stages of virus infection [26]. Fetal hepatocytes are important in Thy-1^{+} human and mice [28, 29]. However, human Thy-1 is not generate in T cells begining in thymus, which differs from mouse T cells [30]. Thus, the original B-1 cells can generate ATA B cells in the thymus of mice [10] but not in human. However, Thy-1 is continuously important in human and mice with Thy-1 expressed on nerve cells (neuron) in brain, fibroblast, endothelial cells, monocytes, myeloid cells, and kidney [30–32], and serum Thy-1 is present. Thy-1 moves to endothelial cell to control the initial state of virus infection, and CD11b (Mac-1) helps to Thy-1 activated to endothelial move [33]. In humans, this CD11b is mostly expressed by neutrophils/monocytes (CD11b^{+}Gr-1^{+}) to move Thy-1 to endothelial tissues [33, 34]. Since Thy-1 is important in the nervous system of mice and human, when lacking Thy-1 in brain, strongly inhibited in the dentate gyrus [35]. Mouse thymocyte autoantibodies from ATA B1 cells react with Thy-1 in thymus, then original peritoneal cavity pB1a with increased CD11b but not in spleen B1a, and in old age CD11b^{+}ATA B cells, and then, ATA B cells exhibit multiple specificites [36].

Mouse ATA B cell lymphoma/leukemia express high levels of Hamp2^{++} which is hepcidin. Hepcidin is found as Hamp1 and Hamp2 in mice, and human hepcidin is similar to mouse Hamp1 [37]. Hepcidin is an innate antimicrobial agent that is induced by most invasive bacteria

Hayakawa *et al. Immunity & Ageing*   (2024) 21:22

Page 3 of 24

and also by virus, then limits bacterial proliferation by reducing iron such as in plasma and extracellular fluids, and kills bacteria [38]. Hamp2 is more reactive as an antibacterial and antivirus activity than Hamp1 [39, 40]. The most important function of hepcidin (also mouse both Hamp1 and Hamp2) is to regulate iron [41]. Hepcidin is mostly produced by macrophages/monocytes, and TLR induced hepcidin by T cells and B cells [42]. ATA B cell tumors in old aged show high Hamp2 expression and decreased iron. This mouse ATA V8-12 V_H is related to human V2-5 which is also cancer related with hepcidin$^+$ or iron$^+$ (Fig. 5D). V_H8-12/V_K21-5 generated in ATA B1 cells, and previously shown V_H8-12/V_k19-17 generated in MZ B cells. Here, we show that this MZ B cells induces the generation of high macrophages in spleen with intestine/colon tumor in old age. Thus, expression of V8-12 in mice is related to B-1 cells with CLL, and cancers with Hamp2^{++} iron^{low} in old age, and V8-12 B-2 MZ B cells increased generation of macrophages with tumor generation in old age.

Results and discussion

CD11b^{++} B CLL/lymphoma develops in old age of mice from B-1 origin V_H8-12/V_k21-5 ATA Tg-expressing cells. Mouse V8-12 homologous to human V2-5

As previously shown (Fig. 1A), expression of V_H3609(V_H8-12)/V_k21-5 transgene (ATAμκ Tg) in the PreB/immature stage drives positive V_H8-12/V_k21-5 selection in B-1 cells through a process involving Arid3a-driven fetal/neonatal B-1 cell development to induce mature CD5$^+$ B1a cells and constitute B1a cells in adults [43]. In adult B cell development from BM (B-2), the expression of V_H8-12/V_k21-5 BCR in immature B cells drives negative selection at the mature B cell stage, resulting in arrest [11]. As shown in Figure S1A, at the 2 mo stage of ATA B cell development, the PerC, mLN, and intestinal PP cell populations were mature B1a, but BM and Spl cells were dominantly immature. ATA B cells in PBL are immature at 2 mo, but an increased fraction of mature are at 8 mo, which corresponds with increased serum IgM, IgG1, IgG3 by 12 mo of age, whereas IgA is already high by 2 mo. However, when Pla2g2a was deleted at the neonate stage, the generation of mature

ATA B cells was reduced including through 14 mo of age [12] (Fig. S1A). Thus, ATAμκTg B cells originally generate neonatal ATA B cells pB1a increase in PBL as mature in middle age and old age. The original anti-thymocyte/Thy-1 autoreactive mAbs from these B cells are polyspecific and can also bind multiple tumor antigens [36].
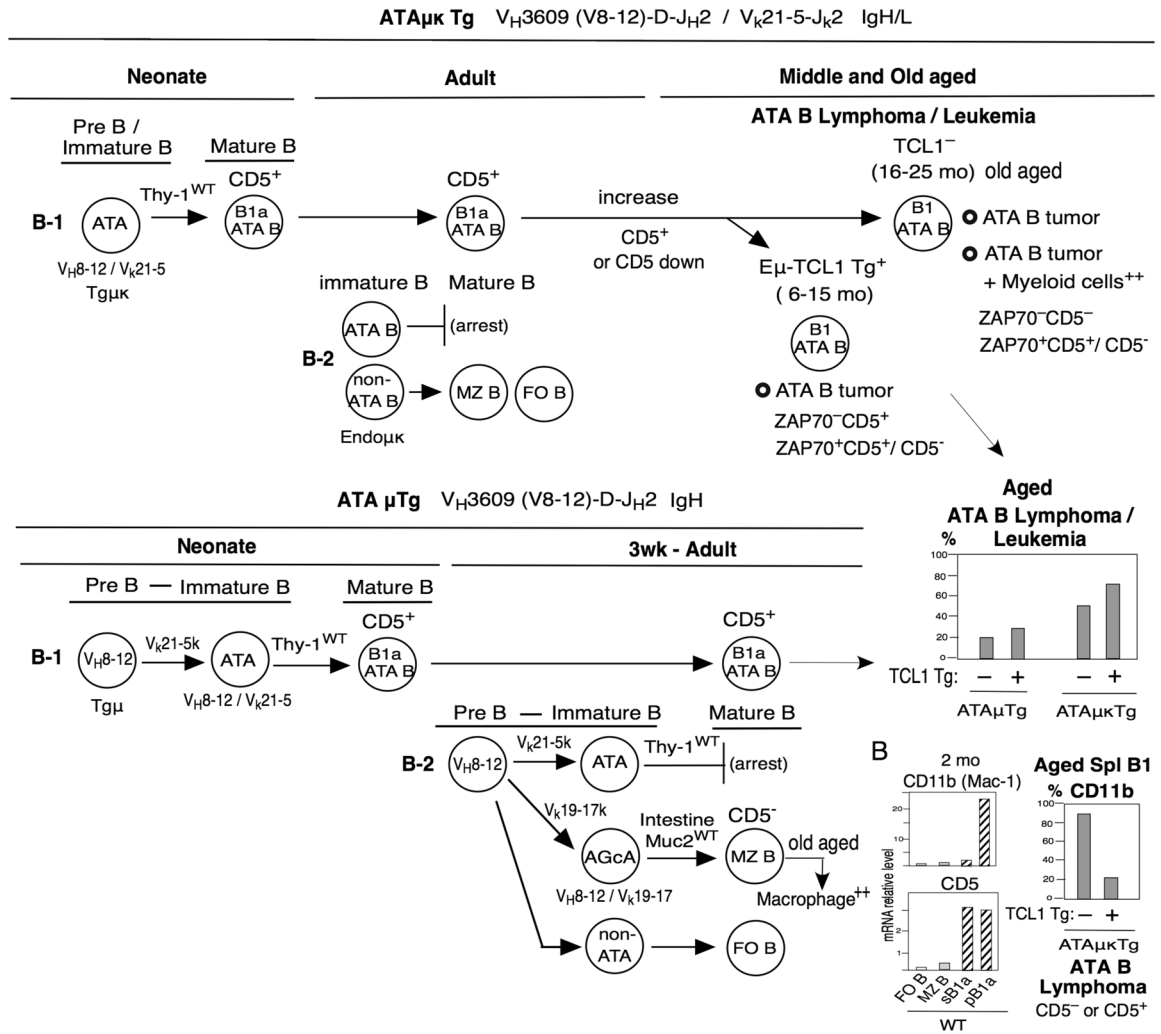
CD5 recruits the SHP-1 protein tyrosine phosphatase to inhibit BCR signaling [20, 21]. Thus, CD5$^+$ B1a cells have more anti-apoptotic signals, serve as a source of autoantibodies, and are considered innate lymphocytes [44]. The Lyn-CD22-SHP-1 pathway promotes BCR tolerance [45]. CD11b also regulates BCR by binding to CD22 [46]. Macrophages in peritoneal cavity can induce B1a cells into PerC [47], which are mainly CD5$^+$CD11b$^+$. When these PerC B1a cells move to spleen, complement component C3 in spleen can decrease CD11b expression as CD11b$^-$ [48], but CD5 expression, thus autoantibody production are retained. However, LPS or CpG can downregulate CD5 in adult B1 cells to generate CD5$^-$ B1 cells [24] (Fig. S1B). These CD5$^-$CD11b$^-$ B1 cells in spleen exhibit strong BCR signaling. In middle age, both TCL1$^-$ (TC$^-$) and TCL1$^+$ Tg (TC$^+$ Tg) ATA B cells can become CD5$^+$ or CD5$^-$, although TC$^-$ ATA B cell tumors are most CD5$^-$, TC$^+$ Tg ATA B cells are mostly continuously CD5$^+$ (Fig. S1B). The TC$^+$ Tg ATA B cells generate lymphoma/leukemia at middle age [24], whereas TC$^-$ ATA B cell tumors are in old age. In older humans, TC$^+$ CLL can develop, in which most tumor cells are CD5$^+$. However, 7–20% human CLL B cells are CD5$^-$ [49], and these human CD5$^-$ B cells induce splenomegaly [50], which is consistent with increased splenic CD5$^-$ B1 cells in the mice.

Mouse TC$^+$ Tg expressing ATA B cells generate slightly more lymphoma/leukemia in middle age than TC$^-$ cells (Fig. 1A). However, TC$^-$ ATA B tumor cells in old age showed the recovery of increased CD11b expression (Fig. 1B) [13] and react with CD22 (shown in Fig. 5C). At 2 mo age, CD11b$^-$ splenic B1a cells stimulated with CpG increased expression of CD11b (or LPS, but low), and the combination of CpG with IL-10 further increased CD11b [13] (Fig. S1C). As previously showed (in Figure S1C), splenic aMyIIA V_HQ52 B1 cells and aPtC V_H11 B1 cells (V_H knock in)

(See figure on next page.)
Fig. 1 Summary of B-1 ATA B and B-2 AGcA cell generation, and mouse V_HV8-12 similar to human V2-5. **A** and **B** V_H8-12/V_k21 ATAμκ Tg mice generate B-1 ATA B cells in fetal/neonate stage and generate CD5$^+$B cells as B1a, differently, negative selection (arrest) occurs during adult B-2 development. B-1 ATA B cells increase in PBL in middle age, and CD5 down can occur or continuous CD5$^+$. In old age CLL/lymphoma generation, CD5$^-$ cells mostly not increased ZAP70, and increased ZAP70 with CD5$^+$ ATA B cells. TC$^-$ (CD5$^-$ and CD5$^+$) increased CD11b (61/73=84%) in CLL/lymphoma, in contrast, Eu-TCL1$^+$ Tg cells generated at middle aged CLL/lymphoma are few increased CD11b (13/60=22%) [13]. V_H8-12 ATAμTg mice can generate V_H8-12/V_k21 B1a and generate CLL/lymphoma in old age (low), and V_H8-12/V_k19 generate MZ B cells and V_H8-12/V_k19μκTg mice generated at 3 wk MZ B cells in B-2 and in old aged generate macrophage^{++}. **C** Mouse V8-12 VH check with human VHs from UniProt and IMGT. Mouse V8-12 V_H gene is similar to human V2-5
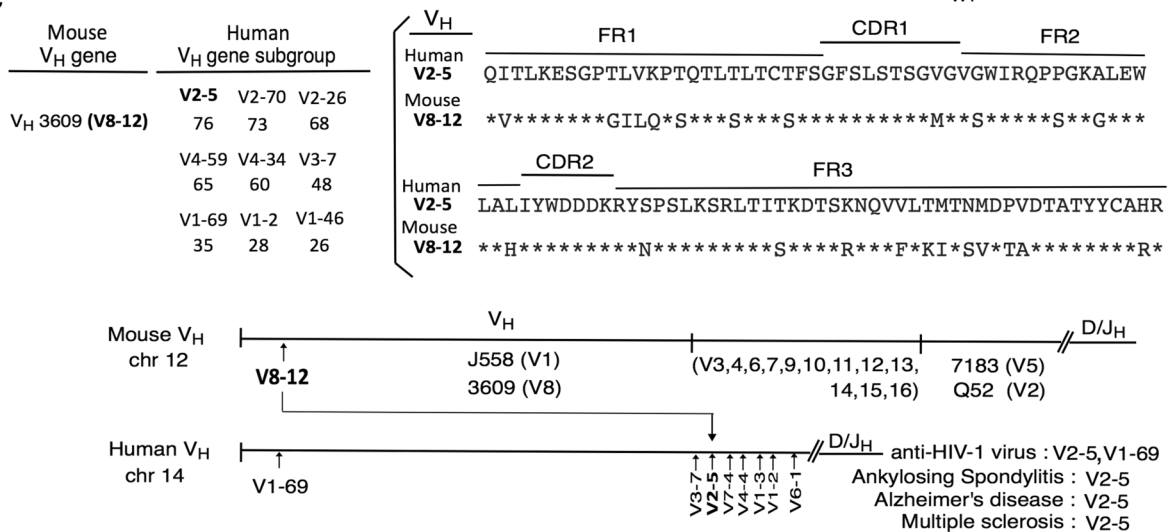
A

ATAμκ Tg V_H3609 (V8-12)-D-J_H2 / $V_κ21$-5-$J_κ2$ IgH/L

Neonate	Adult	Middle and Old aged

ATA B Lymphoma / Leukemia

Pre B / Immature B   Mature B CD5+

$TCL1^-$ (16-25 mo) old aged

B-1 (ATA) →$Thy-1^{WT}$→ (B1a ATA B) → increase / CD5+ or CD5 down → (B1 ATA B) ○ ATA B tumor ○ ATA B tumor + Myeloid cells++

V_H8-12 / $V_κ21$-5 Tgμκ

$ZAP70^-CD5^-$ $ZAP70^+CD5^+/ CD5^-$

immature B   Mature B

B-2 (ATA B) ⊣ (arrest)   (non-ATA B) → (MZ B) (FO B)

Endoμκ

Eμ-TCL1 Tg+ (6-15 mo)   (B1 ATA B)

○ ATA B tumor $ZAP70^-CD5^+$ $ZAP70^+CD5^+/ CD5^-$

ATA μTg V_H3609 (V8-12)-D-J_H2 IgH

Neonate	3wk - Adult

Pre B — Immature B   Mature B CD5+   CD5+

B-1 (V_H8-12) →$V_κ21$-5k→ (ATA) →$Thy-1^{WT}$→ (B1a ATA B) → (B1a ATA B)

Tgμ V_H8-12 / $V_κ21$-5

Pre B — Immature B   Mature B

B-2 (V_H8-12) →$V_κ21$-5k→ (ATA) ⊣$Thy-1^{WT}$ (arrest)

→$V_κ19$-17k→ (AGcA) → Intestine $Muc2^{WT}$ → $CD5^-$ (MZ B) → old aged → Macrophage++

V_H8-12 / $V_κ19$-17

→ (non-ATA) → (FO B)

Aged ATA B Lymphoma / Leukemia

%

TCL1 Tg: − +   − +
           ATAμTg   ATAμκTg

B

2 mo
CD11b (Mac-1)

mRNA relative level

CD5

FO B MZ B sB1a pB1a
WT

Aged Spl B1 % CD11b

TCL1 Tg: − +
ATAμκTg

ATA B Lymphoma $CD5^-$ or $CD5^+$

C

Mouse V_H gene	Human V_H gene subgroup		
V_H 3609 (V8-12)	**V2-5** 76	V2-70 73	V2-26 68
	V4-59 65	V4-34 60	V3-7 48
	V1-69 35	V1-2 28	V1-46 26

V_H

	FR1	CDR1	FR2

Human **V2-5**   QITLKESGPTLVKPTQTLTLTCTFSGFSLSTSGVGVGWIRQPPGKALEW

Mouse **V8-12**   *V*******GILQ*S***S***S**********M**S******S**G***

	CDR2	FR3

Human **V2-5**   LALIYWDDDKRYSPSLKSRLTITKDTSKNQVVLTMTNMDPVDTATYYCAHR

Mouse **V8-12**   **H*********N*********S****R***F*KI*SV*TA********R*

Mouse V_H chr 12 V_H ──── **V8-12** ── J558 (V1) 3609 (V8) ── (V3,4,6,7,9,10,11,12,13,14,15,16) ── 7183 (V5) Q52 (V2) ──// D/J_H

Human V_H chr 14   V1-69 ── V3-7 V2-5 V7-4 V4-4 V1-3 V1-2 V6-1 ──// D/J_H

anti-HIV-1 virus : V2-5, V1-69
Ankylosing Spondylitis : V2-5
Alzheimer's disease : V2-5
Multiple sclerosis : V2-5

Fig. 1 (See legend on previous page.)

Hayakawa *et al. Immunity & Ageing*   (2024) 21:22

Page 5 of 24

also increased CD11b expression in old age [13, 25]. PerC B1a cells originate as $CD5^+CD11b^+$, then become $CD5^+CD11b^-$ upon migration to spleen, then further to $CD5^-CD11b^-$, and middle aged CD11b increased, then, $CD5^-$ $CD11b^{++}$ tumor cells develop in spleen from ATA B cells in old aged mice. In human TC^+CD5^+ CLL, 18% of tumor cells are $CD11b^+$ but most are $CD11b^-$ [51], which differs from the TC^- mouse. Some mouse TC^- ATA B cells progress to lymphoma/leukemia at old age together with increased myeloid cells [13] (Figs. 1A and 5E), which is consistent with some human CLLs that develop with myeloid cells [52, 53].

In ATAμTg (V_H8-12/D/J_h2) mice, $CD5^+$ B1a ATA cells generated lymphoma/leukemia in old age, but at a lower rate than ATAμκTg mice [24] (Fig. 1A). Mice co-expressing V_H8-12 and V_k19-17/J_k1 (as V_H8-12/V_k19-17) generated strong MZ B cell development, and some V_H8-12 FO B cells were also generated [54]. The V_H8-12/V_k19-17 BCR is a natural anti-intestinal goblet cell work (AGcA), V_H8-12/V_k19-17μTg mice strongly generated MZ B cells [54], and some MZ B AGcA cell-derived tumors in old age (Fig. S3). MZ B cells are the major constituent of the marginal zone, together with myeloid, dendritic, and stromal cells [55]. Generally, macrophage/neutrophils $CD11b^+Gr$-1^+ cells generate hepcidin to control iron [56], and also hepcidin^{low} iron$^+$. Then, old aged in AGcA Tg mice generated high macrophage ($CD11b^+Gr$-1^+) (Fig. 1A), and as showed in Fig. 5E and Fig. S3, this macrophages made strong intestine/cold tumor in old aged, not hepcidin related positive, rather iron$^+$ increased.

The mouse V_H8-12 BCR is homologous to human V2-5 (Fig. 1C). Human V1-69 is expressed in unmutated CLL (U-CLL), but V2-5 is low in CLL [57, 58]. Although human V2-5 is very low in cord blood [59], in depth analysis showed V4-59, V4-34, and V2-5 in cord blood [60], suggesting that V2-5 reacts in neonates. Importantly, it is also well known that HIV-1 (human immunodeficiency virus) is associated with increased V2-5 (2F5) and V1-69 (4E10) in humans [61] (Fig. 1C). V2-5 is also found in Ankylosing Spondylitis (AS) [62] and Alzheimer's disease (AD) [63, 64]. AD was also found to be associated with mouse V8-12 as human V2-5 [65]. Then, it has long been known that dominant V2 (most V2-5) expression is associated with increased susceptibility of multiple sclerosis (MS) as brain-gut axis with iron$^+$ [66]. Several cancers in human have used V2-5 as listed in Fig. 5D. V2-5 immunoglobulin are variable, most hepcidin$^+$ and some showed hepcidin^{low} iron$^+$. Thus, in this paper, first mouse TC^- ATAμκ Tg lymphoma/leukemia compared to human old aged TC^+ CLL/U-CLL, and TC^+ ATAμκ Tg middle aged may difference from TC^- in old aged. Then, since TC^- ATAμκ Tg B cells found Hamp2^{++} generated in old age different from human CLL, thus, checked with human V2-5 positive cancers with hepcidin$^+$ or some iron$^+$ lists (Figs. 4 and 5).

Rag1KO Thy1KO ATAμκTg mice generate ZAP70$^+$CD5$^-$ATA B-CLL/lymphoma at early mature and middle age

Previously shown Fig. 2A,B,C. Neonate ATAμκTg mature ATA B cells arise first in the peritoneal cavity (PerC) with the support of macrophages [47] and pleural cavity, and present in spleen, intestine, mLN, LN, liver, and blood of aged mice, which also exhibit strong ATA IgM in serum and plasma cells [11]. ATA B cell tumors in old aged mice are Spl^{++}, mLN^{++}, LN^+, and $Liver^{++/+}$ [13]. In intestinal microbiota, ATA IgM is present in intestine and highest in colon (Fig. 2A). At 2 mo, mature B1 cells are already present in PerC, mLN, and intestinal Peyer's patches (PPs) (Fig. S1). In contrast, as previously shown, in Thy-1KO ATAμκTg mice, the original ATA Tg does not generate $CD5^+$ B1 cells, rather, B-2 non-ATA B cells are increased [55] (Fig. 2B). Rag1KO ATAμκTg mice engineered, mature T and non-ATA B cells were not generated, however, MZ ATA B cells are strongly generated and also ATA B1 cells, both of which are $CD5^-$ [55] (Fig. 2C).

ATAμκTg mice with both Rag1KO and ThyKO background also generated B1-CLL/lymphoma at mature and middle age without CD5 expression, and these tumors expressed higher levels of ZAP70 than TC^- or TC^+ ATAμκ Tg mice, which are most $CD11b^-$ (75%) (Fig. 2D). These tumors express cyclin D2, cMyc, and CTLA-4 as high as originally generated initial B1 cells. Although CTLA-4 is associated with higher CD80 than CD86 in normal mouse B1a cells [67], ZAP70^{hi} RagKOThy1KO mice showed higher CD86 than CD80 and also increased CD24 expression. Mature T cells and non-ATA B cells are absent in Rag1KO mice, but NK and ILC cells and myeloid cells are continuously present. TC^-CD5^-B1 ATA B cells with most $CD11b^-$ are generated with ZAP70^{++} at early age including BCR signaling and found in high numbers in spleen and liver but not in mLN. These early RagKOThy1KO ATA B cell tumors are different from Rag$^+$Thy1$^+$ATA B cells, which are generated at the neonate stage and adult animals controlling tumor development with the presence of mature B-2 and T cells together with Thy-1$^+$, but tumors still develop in old age.

Decreased Nod1, IL5R, CD1d, and increased CD11b in the B1 cells in old aged CLL

Neonate-generated B1a cells are known to express high levels of Nod1 and remain continuously Nod1$^+$, as compared to the low levels in B-2 generated cells [68] (Fig. 3A). These B1a cells are also slightly higher in TLR7 and TLR9 than FO B at 2 mo (Fig. 3A). When FO B and pB1a cells were stimulated, FO B cells were found
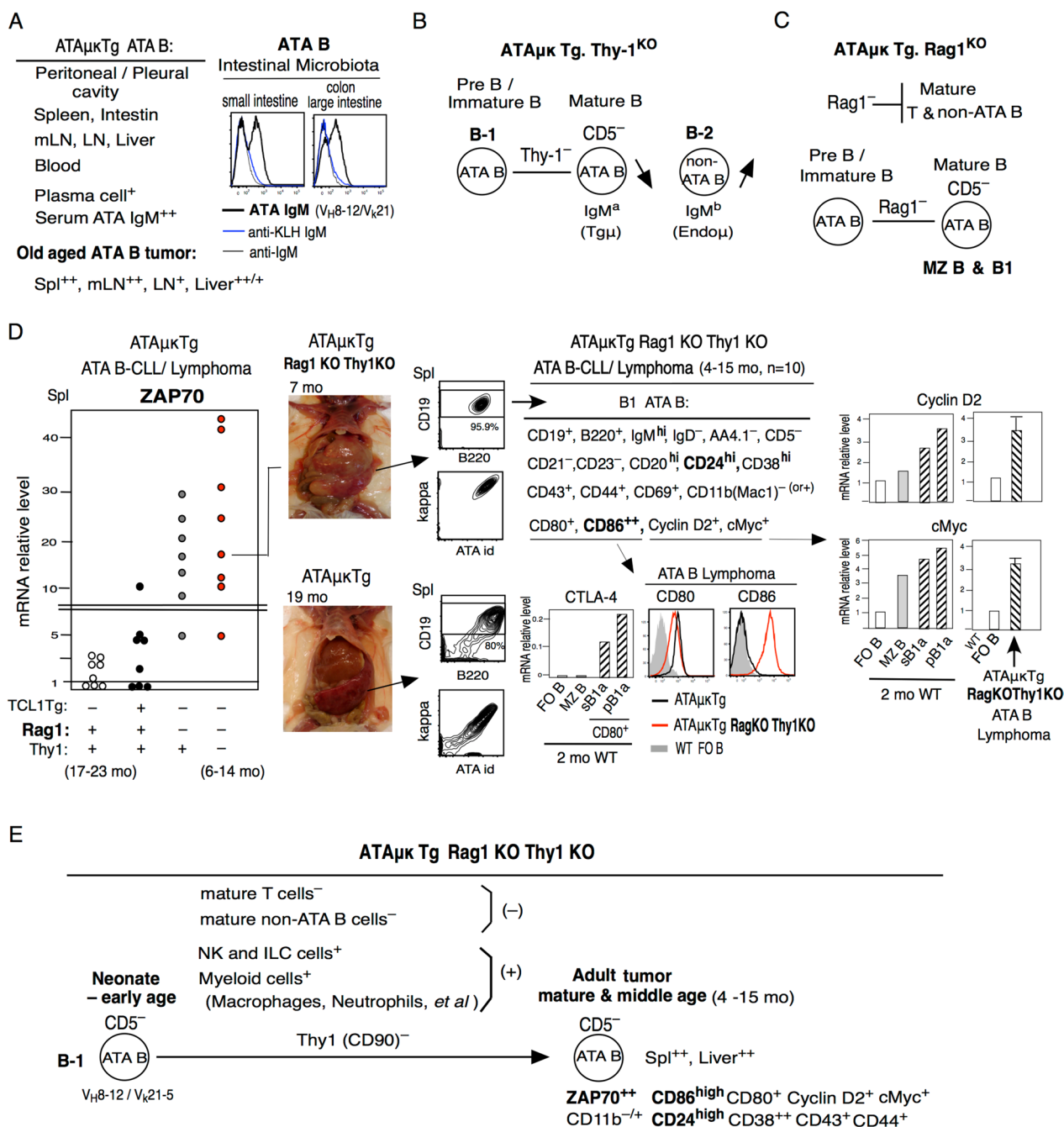
Hayakawa *et al. Immunity & Ageing*   (2024) 21:22

Page 6 of 24

Fig. 2 Rag1KOThy1KO ATAμκTg mice generate mature &middle age ATA B tumor. **A** Summary of ATAμκTg ATA B generation and old aged ATA B tumor place. ATA B IgM react with intestinal microbiota, and higher in colon, a-IgM is the control. **B** and **C** Summary of ATAμκTg with Thy-1[KO] or Rag1[KO]. Thy-1[KO] showed decreased B-1 ATA B cells with CD5^{-}, rather B-2 non-ATA B cells increase. Rag1[KO] showed increased MZ B and B-1 ATA B, and both not generated CD5. **D** and **E** ZAP70 levels in ATA B-cell/lymphoma generation in TC[-], TC[+], TC[-]Rag1[KO], and TC[-]Rag1[KO]Thy-1[KO] mouse levels with negative FO B as set to 1.0. TC[-]ATAμκTg Rag1[KO]Thy-1[KO]ATA B mice highest ZAP70, and generated early (mature & middle) age ATA B-cell/lymphoma generation. High CD86 and high CD24 are different with old age most TC^{-}ZAP70^{-}CD5^{-} ATAμκTg mice, but cyclin D2 and c-Myc are continually high as TC^{-}ATAμκTg mice

to express high levels of ZAP70 mRNA by anti-IgM, but this did not occur in B1a cells (Fig. 3A) since CD5 expression in B1a does not require BCR signaling. However, combining CiE-DAP for Nod1 reaction with anti-IgM increased ZAP70 expression, but not Nod2, in B1a cells also in FO B. Treatment with TNFa increased ZAP70

Hayakawa *et al. Immunity & Ageing* (2024) 21:22

Page 7 of 24

expression in both B1a and FO B, and further increases ZAP70 when TNFa was combined together with Nod1 expression. Nod1 is important for B1a cell increase, since at 4 mo, Nod1$^{-/-}$ are low ATA B cells in ATAμκTg mice. In addition to Nod1, IL5 is also required for B1a cell generation and maintenance in contrast to FO B cells [69], and expression of CD1d is essential for NKT cell reactivity are similar between B1a and FO B cells as previously shown [12]. ATA B CLL generated at middle age is continuously Nod1$^+$, IL5R$^+$ and CD1d$^+$, also in the presence of TC$^+$Tg. In TC$^-$ ATA B cell tumors, expressions of these decreased in old aged mice [12] (Fig. 3B). Compared, CD11b expression is increased on CLL developing in middle aged spleen, and further increased on tumors at old age [12, 13] (Fig. 3C). Original B1a cells at 2 mo express more CXCR5 than CXCR4, whereas TC$^-$ATA B cell tumors at old age showed decreased CXCR5 and increased CXCR4, as compared to TC$^+$Tg mice (Fig. 3C). Similarly, in aged humans, CLL that arises CXCR4 expression higher than CXCR5 [70].

We next performed microarray gene expression analysis of tumor to compare TC$^-$ versus TC$^+$ Tg ATA B cells and ZAP70$^-$ versus ZAP70$^+$ cells in Fig. 4A, B. We also compared gene expression in CD5$^-$ vs CD5$^+$ ATA B1 cells from 12 mo TC$^-$ ZAP70$^-$ mice in Fig. 5A.

Increased ZAP70 expression in TC$^+$ mice as in TC$^-$ mice are similar to human CLL/U-CLL, however, old aged TC$^-$ATA B cell tumors increased than middle age TC$^+$

Gene expression in ATA B cell tumors compared between old aged TC$^-$ZAP70$^-$CD5$^-$, TC$^-$ZAP70$^+$CD5$^+$, vs middle aged TC$^+$ZAP70$^-$CD5$^+$ mice (Fig. 4A), and between TC$^-$ZAP70$^-$CD5$^-$ vs TC$^+$ZAP70$^+$CD5$^+$ mice (Fig. 4B). Nod1 expression was decreased in old aged TC$^-$ tumor cells, and T-bet and CD11c were increased. T-bet$^+$CD11c$^+$ are consistent with old aged in humans [71, 72]. Tumor from TC$^-$ZAP70$^-$CD5$^-$ mice expressed the highest levels of CD11b and cyclin D2, and TC$^+$ (both ZAP70$^-$ and ZAP70$^+$) ATA B cells lacked CD11b, but TC$^+$ZAP70$^+$ increased cyclin D2 (Fig. 4B2, B1). Normal B1a cells show higher levels of cyclin D2 than FO B cells

(Fig. 2D), and cyclin D2 is expressed in human CLL [73]. Since CB.70 mice have a p16^{INK4a} mutation [74], cyclin 2 (G1) expression can be more increased, and promote moving from G1 to G2/M [75]. Then, both ZAP70$^+$ with TC$^-$ and TC$^+$ are higher in cyclin D1 (G1), cyclin E1 (G1/S), cyclin A2 (G2/M) (Fig. 4A1, B1) (also higher cyclin D3 and cyclin B1 (G2/M); data not shown) by p16^{INK4a} mutation.

ZAP70$^+$ tumor under both TC$^-$ and TC$^+$ genotypes exhibited increased expression of TNFa, CD40, IL4, several Tubb (β-tubulin) genes, cMyc, Fzd2, Ki67, and CD86 (Fig. 4A1, B1). Among the Tubb genes, WT fetal/neonatal B1a are higher in Tubb6 [76], and all B cells are positive for Tubb5 [77]. Tubb5 is high in TC$^+$ZAP70$^+$ tumor, but Tubb6 is higher in both TC$^-$ tumors, as compared to TC$^+$ tumor (Fig. 4A1,B3). cMyc was also originally higher in B1a cells (Fig. 2D) and ZAP70$^+$ increased as human U-CLL than M-CLL. Fzd2 is β-catenin dependent, and human CLL and ZAP70$^+$ U-CLL showed expression of Wnt10a and Wnt6, which generated Fzd2 [78]. Ki67 (NKI67) is a proliferation-related antigen. High Ki-67 index is associated with many cancers, and human CLL ZAP70$^+$/U-CLL are also Ki67^{hi} [79]. We also found that CD86 expression was higher than CD80 in ZAP70$^+$ tumors (Fig. 4A1 and B1), which was also found in ATAμκTg Rag1KO Thy1KO mice that are ZAP70^{++} (Fig. 2D). As in Figs. 4B1, human U-CLL are most similar to ZAP70$^+$ TC$^-$ and TC$^+$ tumors as increased CD40, IL-4, cMyc, Fzd2, Ki67 (see Fig. S4-1 for human CLL/U-CLL references). Since human CLL with normal p16^{INK4a}, human CLL expression of cyclin D1 is limited, and cyclin A2 is not increased, and CD86$^+$ cells are only small portion of the CLL [80].

TC$^+$ZAP70$^+$ also increased as in TC$^-$ cells including TC$^-$ZAP70$^-$ cells (Fig. 4B2). B1a cells showed slightly higher TLR7, TLR9, and TLR4 expression than FO B cells at the 2 mo stage. As intracellular Nod1 is decreased in old aged, TC$^-$ promote TLR7 and TLR9 increases (Fig. 4A2), and TC$^+$ZAP70$^+$ cells also showed increased TLR7 (Fig. 4B2). In contrast, middle aged TC$^+$Tg tumor cells are strongly high for TLR4 (Fig. 4A2).

(See figure on next page.)

Fig. 3 Nod1 is important in early B1a cells and Nod1, IL-5R, CD1d decrease in old aged and increased CD11b and CXCR4, different from middle aged TC$^+$Tg ATA B cells. **A** Nod1 high in neonate and adult B1a. 2 mo FO B versus pB1a for ZAP70 generation after 20 hour later by anti-IgM without or with CiE–DAP (Nod1) or MDF (Nod2), or TNFa without or with CiE-DAP. ZAP70^{hi} in a-IgM is only FO B cells not CD5$^+$pB1a, but Nod1 add increased ZAP70. Down: 4 mo ATAμκ Tg mice with NOD1$^{+/-}$ or NOD1$^{-/-}$. ATAid is originally generated V$_H$8-12/V$_K$21-5, then, low ATA B cells in Nod1$^{-/-}$. Thus, Nod1 is important. **B** Nod1, IL-5R, CD1d comparison between TC$^-$ versus TC$^+$Tg ATAμκTg, in 2 mo and meddle aged leukemia CLL and old aged TC$^-$ CLL/lymphoma. Old aged TC$^-$ tumor showed down these lists, not middle aged TC$^-$ and TC$^+$Tg. **C** Conclusion of TC$^-$ATAμκTg ATA B in 2 mo verus old age tumor stage in spleen, with increased CD11b in TC$^-$ ATA B in flow cytometry analysis. Down: In microarray analysis, TC$^-$ old age ATA B cells are CXCR4 increase versus CXCR5 down, different compared with TC$^+$Tg. Down right: Several TC$^-$ versus TC$^+$Tg ATAuk Tg lymphoma/leukemia pictures used for Fig. 4: 16 mo and 17 mo TC$^-$ZAP70$^-$CD5$^-$ (Spl^{++}, mLM^{++}, LN$^+$), 22 mo TC$^-$ZAP70$^+$CD5$^+$ (Spl^{++}, colon^{++}, LN$^+$), 10 mo TC$^+$ZAP70$^-$CD5$^+$ (Spl^{++}, mLN$^+$, PerC^{++}), 16 mo TC$^+$ZAP70$^+$CD5$^+$ (Spl$^{++,}$ Liver^{++}, PerC^{++}), and 12 mo samples Fig. 5

Fig. 3 (See legend on previous page.)

Hayakawa *et al. Immunity & Ageing* (2024) 21:22

Page 9 of 24
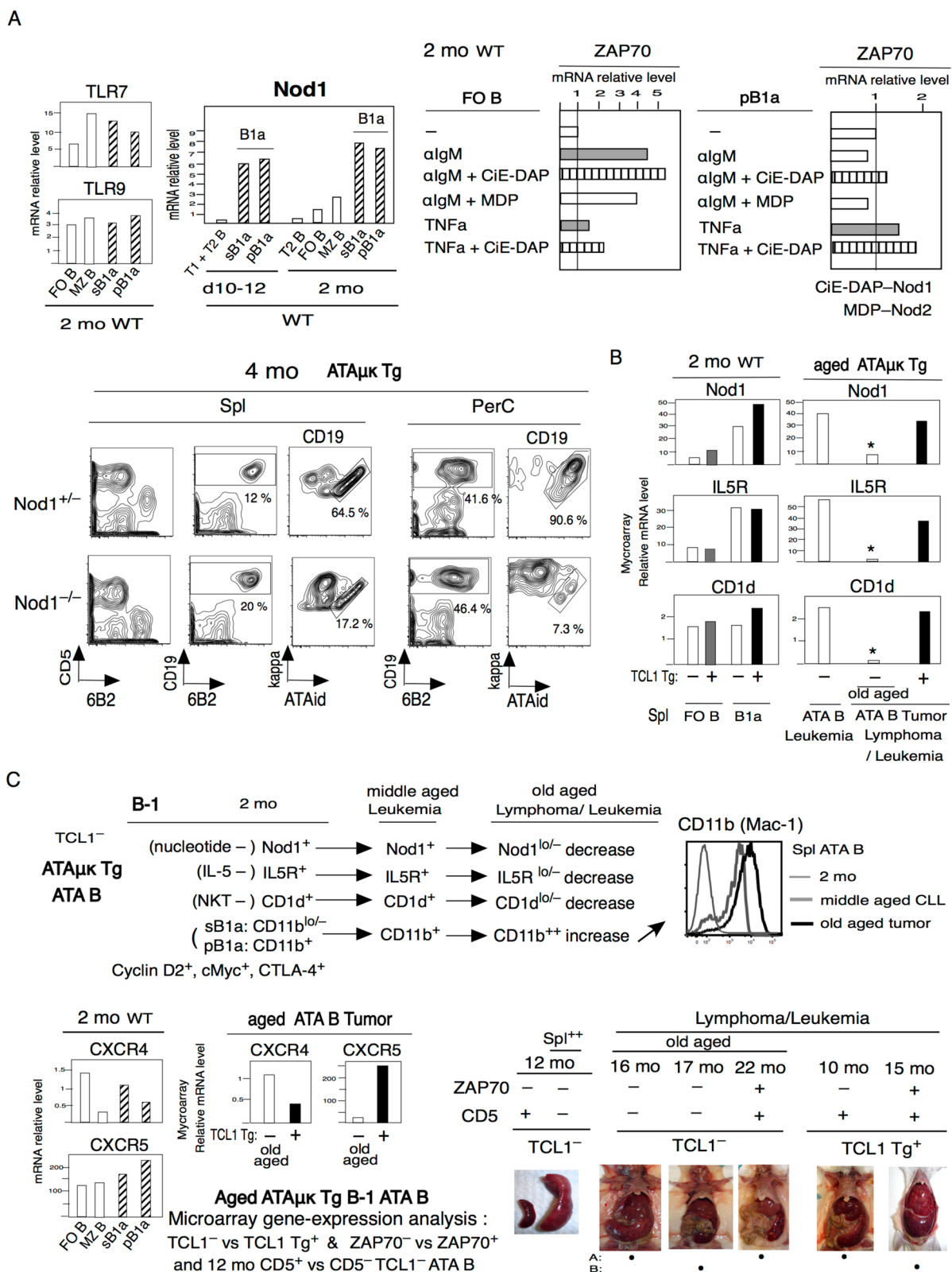
Wnt/β-catenin family members are Wnt1,2,3,8,10 with LRP5/6, and non-β-catenin (Wnt/Ca^{2+}) family members are Wnt 4,5,6,7,11,16 with ROR1/2. TC$^-$ tumors showed dominant expression of Wnt/b-catenin Wnt10b (Fig. 4A2) and also TC$^+$ZAP70$^+$ tumor showed dominant expression of both Wnt10a and 10b (Fig. 4B2). Previous studies showed that human CLL express Wnt3, 4, 5a, 5b, 6, 7, 10, 11, 14, 16 and up-regulated in CLL are Wnt3,5,6,10,14,16 [81]. Wnt5a/5b are the most important in U-CLL [82] and other human cancers also express Wnt5a, whereas Wnt5a was very low in the mouse ATA B tumors. Rather, Wnt5b and Wnt6 were high in both TC$^-$ZAP70$^+$ and TC$^+$ cells (Fig. 4A2, B2). Wnt10 induces expression of Fzd1 and Fzd5, and Wnt5b induces Fzd4 and Fzd6. ROR1 is commonly expressed in human CLL as a component of the Wnt5a-ROR1-ERK1/2 pathway [83], however, mouse TC$^+$ ATA B tumors showed very low ROR1, but instead expressed ROR2. Higher in TC$^-$ZAP70$^+$ and TC$^+$ZAP70$^+$ increased Wnt5b–ERK2, also in human U-CLL [54]. Myd88 generated from TLRs and higher in TC$^-$ with TLR7, 6 (Fig. 4A2), then, increased Myd88 in TC$^+$ZAP70$^+$ cells occurred together with TLR7 increase (Fig. 4B2). TC$^-$ZAP70$^-$CD5$^-$ showed increased STAT3, IL-10, IL-6 more than TC$^-$ZAP70$^+$CD5$^+$, and TC$^+$ZAP70$^+$CD5$^+$ cells showed increased these (Fig. 4B2). Thus, middle age TC$^+$ZAP70$^+$ increased as in some TC$^-$ cells (including TC$^-$ZAP70$^-$CD5$^-$) than TC$^+$ZAP70$^-$. TC$^-$ positive cells and increased TC$^+$ZAP70$^+$CD5$^+$ in ATA B tumor are the most similar to human CLL data, and CD44^{++} Ki67$^+$ as ZAP70$^+$ higher (also TC$^-$ ZAP70$^-$ positive) are significant in U-CLL (Fig. 4B2, References in Fig. S4-2).

In TC$^+$ (ZAP70$^-$ and ZAP70$^+$) ATA B cells, TLR4, Wnt5b/Wnt6, and Fzd6, Rac2 showed high positive than TC$^-$, and Runx2, NF-kB, p300 were also high (Fig. 4A2). Runx2 and p300 are NF-kB generation [84, 85]. Then, TC$^+$ showed high APRIL, contrast to TC$^-$ showed high BAFF. Tuft1 (tuftelin) is multiple cancers as metastasis, and up-regulating the Rac1/β-catenin pathway [86]. Tuft1 can induce NF-kB [87], and TC$^+$ showed high Tuft1 than TC$^-$ cells. Although Wnt5a/b from the origin as non-β-catenin, however, Wnt5a/b can be changed to binding to β-catenin [88, 89], thus Wnt/b-catenin-TCF/LEF binding can occur. TC$^+$ showed LRP5$^+$ (different to TC$^-$LRP6$^+$)

and high LEF1 than TC$^-$ (both ZAP70$^-$ and ZAP70$^+$) (Fig. 4A2, B2).

CD38, CD43, CD44 in B1a cells are originally higher than FO B cells (Fig. S2B), and increased these in old aged TC$^-$ tumor than meddle aged TC$^+$ cells, as also shown in flow cytometry analysis (Fig. 4A3). CD38 is different from human than mice, since human FO B cells are negative, then GC B cells increased CD38 [90], and human U-CLL showed high CD38^{++} and CD44^{++} [91, 92]. Since high CD44^{++} in human ZAP70$^+$ CLL, CD44 is the highest in TC$^-$ZAP70$^+$ than TC$^-$ZAP70$^-$, and also TC$^+$ZAP70$^+$ increased (Fig. 4B2). CD43 showed human CLL positive [93], as found in mouse TC$^-$ tumor. TC$^+$ showed higher CD21, CD23, CD24, CD27, and CD49d than TC$^-$. CD21 and CD23 are original low/negative in PerC B1a cells, and TC$^-$ ATA B tumor were similar low/– and increased in TC$^+$ ZAP70$^-$ cells (but, TC$^+$ZAP70$^+$ down). Human U-CLL can be CD21^{low} [94], and some CLL also showed low CD23 [95]. CD24 are all normal B cells$^+$ and increased CD24 have been known for cell growth/cancer [96], and increased CD24 was found in TC$^-$Rag1KOThy1KO mice in mature &middle aged ATA B tumor (Fig. 2D), then, old aged TC$^-$ showed decreased (Figs. 4A3 and 5D). CD27 are low/– for all normal B cells compared to CD27$^+$ T cells in mice, and TC$^+$ cells (ZAP70$^-$ and ZAP70$^+$) showed slightly increased CD27. In human CD27 are different from mice, since human CD27 are positive in B cells, and original early human B1 cells are CD27$^+$ [97] and CLL CD27$^+$ [98], however, U-CLL can become CD27$^{low/-}$ by principal component analysis [99]. CD49d are all B and T cells positive, and increased in TC$^+$ Tg cells, in comparison, TC$^-$ cells showed down regulated CD49d (Fig. 4A3). Most human CLL are CD49d$^+$, however few human CLL can became down regulated CD49d in age [100]. These CD case papers in TC$^-$ > TC$^+$ and TC$^-$ < TC$^+$ are also listed in Fig. 5A.

Although ZAP70$^+$ increased in TC$^+$ cells as in TC$^-$ cells similar to old aged human CLL and U-CLL, many showed increased old aged TC$^-$ cell tumor than middle aged TC$^+$ cells (Fig. 4B3), incruding Hamp2 increased in TC$^-$. It is possible that TC$^+$ > TC$^-$ data could be for TC$^-$ decrease in old aged. Thus, next in Fig. 5, 12 mo TC$^-$ cells analysis with normal CD5$^+$ ATA B mice versus CD5

(See figure on next page.)
Fig. 4 Microarray mRNA analysis by ATA B lymphoma/leukemia. TC$^-$ZAP70$^-$CD5$^-$, TC$^-$ZAP70$^+$CD5$^+$ vs TC$^+$ZAP70$^-$CD5$^+$ and TC$^-$ZAP70$^-$CD5$^-$ vs TC$^+$ZAP70$^+$CD5$^+$. ATA B in spleen. **A** A1: Higher of TC$^-$ZAP70$^-$CD5$^+$ list. A2,3: higher of TC$^-$ZAP70$^-$ than TC$^+$ZAP70$^-$CD5$^+$ (TC$^-$ >TC$^+$) and higher TC$^+$ZAP70$^-$CD5$^+$ than TC$^-$ (TC$^+$ > TC$^-$) list. A3: add flow cytometry analysis of TC$^-$ versus TC$^+$ ATA B lymphoma/leukemia together with WT FO B cell. **B** B1: TC$^+$ZAP70$^+$CD5$^+$ similar to high TC$^-$ZAP$^+$CD5$^-$ cells. B2: TC$^+$ZAP70$^+$CD5$^+$ also several high TC$^-$ZAP70$^-$CD5$^-$ cells. TC$^+$>TC$^-$ are not listed by genes TC$^+$ZAP70$^+$CD5$^+$ decreased to TC$^-$. B3: TC$^+$ZAP70$^+$CD5$^+$ cells and also TC$^+$ZAP70$^-$CD5$^+$ are not increased to old aged TC$^-$ cells (ZAP70$^-$CD5$^-$, ZAP70$^+$CD5$^+$) as TC$^-$ > TC$^+$

Fig. 4 (See legend on previous page.)

Hayakawa *et al. Immunity & Ageing*   (2024) 21:22

Page 11 of 24
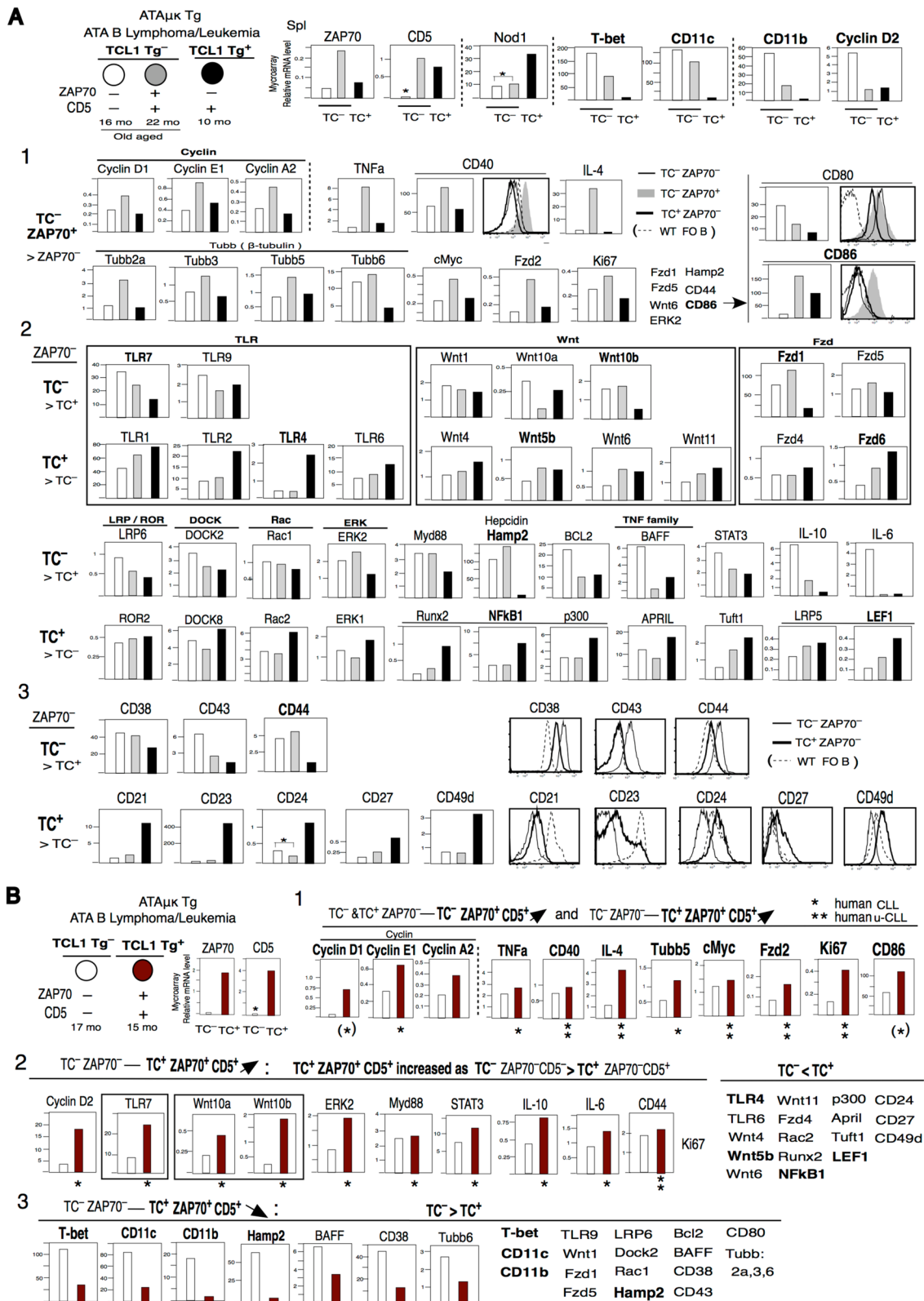
decreased CD5⁻ ATA B mice with spleen increased mice, compare with original Fig. 4 TC⁻ > TC⁺ and TC⁺ > TC⁻ data. Also, further analyses to check with human old aged CLL related, including CXCR.

TC⁻CD5 down ATA B cells with spleen⁺⁺ similar to old aged TC⁻ lymphoma/leukemia. TC⁺Tg ATA B tumor are NF-kB1 increased

Figure 5A and B. Middle age 12 mo ATA B TC⁻ATAμκ Tg mice compared between normal CD5⁺ B1a cells versus decreased CD5 (CD5⁻)B1 cells with spleen increase. This TC⁻12 mo analysis checked with original TC⁻ vs TC⁺ ATA B tumor data in Fig. 4. Further, add microarray analysis about β-catenin/CTNNB1, Damp/HMGB1, CXCR (CXCR4, CXCR5) (also CXCR3 in Fig. S2A), DDP4(CD26), AID, CD1d, and CD180 with original Fig. 4A samples, and TC⁺ZAP70⁺ tumor comparison are in Fig. S2. Under 12 mo TC⁻ZAP70⁻CD5⁻ cell, Nod1, IL5R, and CD1d are decreased similar to old aged TC⁻ATA B tumor, and CTLA4 down as both TC⁻ and TC⁺Tg cells (Fig. S2A) and human CD38⁺⁺ as U-CLL are CTLA4 decreased (Fig. S4-3). This TC⁻ZAP70⁻CD5⁻ cell most similar to increased in old aged increased TC⁻ and TC⁺ZAP70⁺ > TC⁺ZAP70⁻ and TC⁻ > TC⁺ ATA B tumor generation (except low Wnt10a), and similar to low TC⁻ cells than TC⁺ cells.

β-catenin/CTNNB1 and HMGB1 are TC⁻ cells high, and TC⁻ ZAP70⁺ are more higher, and TC⁺ ZAP70⁺ are also increased (Fig. S2A). Damp, as damage-associated molecular patters (tumor promoting, and antitumor effects), present HAGB1 (high mobility group box 1) [101], and Damp/HAGB1 generate TLR pathway (TLR2,4,7,9), also generate CXCL12 with CXCR4 [102]. High β-catenin CTNNB1 and HMGB1 in TC⁻ and TC⁺ZAP70⁺ cells are in human CLL positive and high HMGB1 in CLL plasma [103].

About detail of CXCR in Fig. S2A. CXCR4 is TC⁻ high and TC⁺ low, as TC⁺ZAP70⁺ also low. Then, decreased CXCR5 in TC⁻, and TC⁺ZAP70⁻ with continuously high CXCR5 as original 2 mo B1a cells, however, decreased CXCR5 in TC⁺ZAP70⁺. CXCR3 and CCR7 were also higher in TC⁻ than TC⁺ZAP70⁻, and TC⁺ZAP70⁺ with

decreased CXCR5 showed slightly increased CXCR3 but CCR7 was not increased (Fig. S2A). Thus, TC⁻ATA B tumor showed CXCR4⁺, CXCR3⁺, CCR7⁺ and low CXCR5. In human CLL, CXCR4 higher than CXCR5 [70] different from mouse TC⁺Tg, and CLL also showed CXCR3⁺ [104] and CCR7⁺ in CLL. DPP4⁺ (dipeptidyl peptidase-4)(CD26) are majority of all B cells⁺, and DPP4 also increase CXCR4 [105]. DPP4 are higher in old aged TC⁻ with CXCR4ʰⁱ, and low in middle aged TC⁺ cells (both ZAP70⁻ and ZAP70⁺) as CXCR4 low. Human CLL are high DPP4, and with high DPP4 in serum with U-CLL [106, 107]. AID (activation-induced cytidine deaminase) original in fetal liver [108], and autoreactive B cells in immature B cells (T1/T2 B cells) in B-2 cells are AID⁺, then down for mature FO B, and B1a are also originally low AID (Fig. S2A), then, TLR9 induces AID [109]. In human, U-CLL showed high AID than mutated M-CLL [110], and mouse TC⁻ ATA B tumor in old aged, also showed high AID, not TC⁺ cells (both ZAP70⁻ and ZAP70⁺) (Fig. 5A, Fig. S2A). CD1d and CD180 are decreased in old aged TC⁻ATA tumor, compaired to middle aged TC⁺ (both ZAP70⁻ and ZAP70⁺) (Fig. 5A, Fig. S2A). CD180 is originally increased from immature to mature FO B and MZ B cells, also B1a cells CD180⁺. Then, TLR7,9 signaling pathway significantly downregulate CD180 [111] and mouse old aged TC⁻ ATA B tumor showed the lost CD180. In human old aged CLL, survival mature M-CLL are CD180⁺, contrast to U-CLL are CD180⁻ [112], and aged memory B cells became CD180⁻. Conclusion, TC⁻ > TC⁺ and also down TC⁻ in old age were most similar to 12 mo spleen infection in TC⁻CD5⁻ cells, and these are most similar to old aged human CLL/U-CLL (TC⁻ > TC⁺ samples for human CLL/U-CLL references in Fig. S4-2).

TC⁺ > TC⁻ tumor lists found to be mostly down in 12 mo TC⁻CD5⁻ cells than normal TC⁻CD5⁺B1a. Thus, most TC⁺ tumor appeared to be not increased by tumor than TC⁻. However, 12 mo TC⁻CD5⁻ increased high NF-kB1 and also increased in Runx2 and p300 as similar to TC⁺ > TC⁻. Thus, clearly, TC⁺ cells are more increased NF-kB1 and NF-kB related Runx2 and p300 [84, 85] than TC⁻. In Fig. 5B showed that NF-kB is also

(See figure on next page.)

Fig. 5 12 mo TC⁻CD5 down ATA B spleen⁺⁺ cells similar to old aged TC⁻ATA B lymphoma/leukemia. TC⁺Tg ATA B lymphoma/leukemia are NF-kB1 high. Old aged TC⁻ ATA B are CD11b⁺⁺CD22⁺⁺, CD24ˡᵒʷ, and Hamp2⁺⁺ generation, and V8-12 with Vₖ19 AGcA MZ B are 12 mo Hamp2⁺ and old age generated macrophage⁺⁺ with intestinal tumor. **A** and **B**. 12 mo TC⁻CD5⁻ ATA B with spleen⁺⁺ generate similar to old aged TC⁻CD5⁻ATA B tumor. TC⁺Tg ATA B CLL/lymphoma are higher NF-kB and TCL1 induced miR21 and miR155 and down miR29. **C** TC⁻ lymphoma/leukemia showed CD11b⁺⁺CD22⁺⁺ and generate Hamp2⁺⁺ (TC⁻ZAP70⁻ are more IL10 and IL-6, and TC⁻ZAP70⁺ are high IL-22R) with iron down, as USF2⁺, TFR⁺, FPN⁻. **D** TC⁻ ATA B lymphoma/leukemia generated high Hamp2 and CD44⁺⁺CD24ˡᵒʷ. Human V2-5 positive papers, as kidney, Breast cancer, Pancreatic cancer, SARS-CoV-2, and SLE. Breast cancer are CD44⁺⁺CD24ˡᵒ. **E** Some ATA B tumor showed together with high myeloid cells (CD11b⁺Gr-1⁺) [13], and Vₕ8-12/Vₖ19 AGcA generate MZ B with Hamp2⁺ in 12 mo, then old aged generate macrophages⁺⁺ in spleen with intestine/color tumor⁺⁺
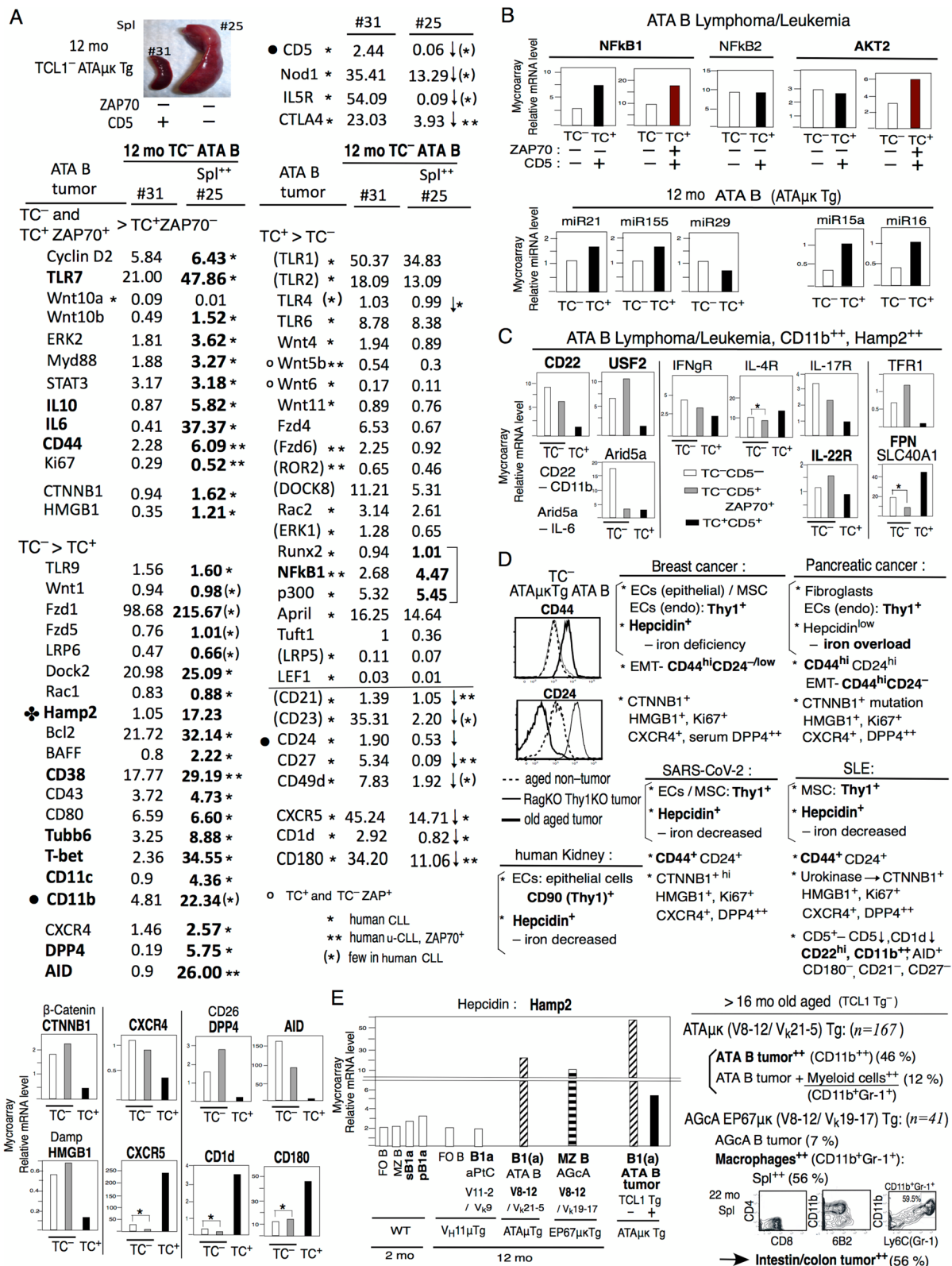
A

Spl #31 #25
12 mo TCL1⁻ ATAμκ Tg
ZAP70 — —
CD5 + —

	#31	#25
● CD5 *	2.44	0.06 ↓(*)
Nod1 *	35.41	13.29 ↓(*)
IL5R *	54.09	0.09 ↓(*)
CTLA4 *	23.03	3.93 ↓ **

12 mo TC⁻ ATA B

ATA B tumor	Spl++ #31	#25
TC⁻ and TC⁺ ZAP70⁺ > TC⁺ZAP70⁻		
Cyclin D2	5.84	**6.43** *
TLR7	21.00	**47.86** *
Wnt10a *	0.09	0.01
Wnt10b	0.49	**1.52** *
ERK2	1.81	**3.62** *
Myd88	1.88	**3.27** *
STAT3	3.17	**3.18** *
IL10	0.87	**5.82** *
IL6	0.41	**37.37** *
CD44	2.28	**6.09** **
Ki67	0.29	**0.52** **
CTNNB1	0.94	**1.62** *
HMGB1	0.35	**1.21** *
TC⁻ > TC⁺		
TLR9	1.56	**1.60** *
Wnt1	0.94	**0.98** (*)
Fzd1	98.68	**215.67** (*)
Fzd5	0.76	**1.01** (*)
LRP6	0.47	**0.66** (*)
Dock2	20.98	**25.09** *
Rac1	0.83	**0.88** (*)
✤ **Hamp2**	1.05	**17.23**
Bcl2	21.72	**32.14** *
BAFF	0.8	**2.22** *
CD38	17.77	**29.19** **
CD43	3.72	**4.73** *
CD80	6.59	**6.60** *
Tubb6	3.25	**8.88** *
T-bet	2.36	**34.55** *
CD11c	0.9	**4.36** *
● **CD11b**	4.81	**22.34** (*)
CXCR4	1.46	**2.57** *
DPP4	0.19	**5.75** *
AID	0.9	**26.00** **

12 mo TC⁻ ATA B

ATA B tumor	Spl++ #31	#25
TC⁺ > TC⁻		
(TLR1) *	50.37	34.83
(TLR2) *	18.09	13.09
TLR4 (*)	1.03	0.99 ↓*
TLR6	8.78	8.38
Wnt4 *	1.94	0.89
o Wnt5b **	0.54	0.3
o Wnt6 *	0.17	0.11
Wnt11 *	0.89	0.76
Fzd4	6.53	0.67
(Fzd6) **	2.25	0.92
(ROR2) **	0.65	0.46
(DOCK8)	11.21	5.31
Rac2	3.14	2.61
(ERK1) *	1.28	0.65
Runx2 *	0.94	**1.01**
NFkB1 **	2.68	**4.47**
p300 *	5.32	**5.45**
April	16.25	14.64
Tuft1	1	0.36
(LRP5) *	0.11	0.07
LEF1 *	0.03	0.01
(CD21) *	1.39	1.05 ↓**
(CD23) *	35.31	2.20 ↓(*)
● CD24 *	1.90	0.53 ↓
CD27 *	5.34	0.09 ↓**
CD49d *	7.83	1.92 ↓(*)
CXCR5 *	45.24	14.71 ↓*
CD1d	2.92	0.82 ↓*
CD180 *	34.20	11.06 ↓**

o   TC⁺ and TC⁻ ZAP⁺
*   human CLL
**   human u-CLL, ZAP70⁺
(*)   few in human CLL

β-Catenin CTNNB1 | CXCR4 | CD26 DPP4 | AID
Damp HMGB1 | CXCR5 | CD1d | CD180
TC⁻ TC⁺

B

ATA B Lymphoma/Leukemia
Microarray Relative mRNA level
NFkB1   NFkB2   AKT2
ZAP70 : — + / — + ; CD5 : — + / — +
TC⁻ TC⁺

12 mo ATA B (ATAμκ Tg)
Microarray Relative mRNA level
miR21   miR155   miR29   miR15a   miR16
TC⁻ TC⁺

C

ATA B Lymphoma/Leukemia, CD11b++, Hamp2++
Microarray Relative mRNA level
CD22   USF2   IFNgR   IL-4R   IL-17R   TFR1
Arid5a   IL-22R   FPN SLC40A1
CD22 – CD11b ; Arid5a – IL-6
□ TC⁻CD5⁻   ▩ TC⁻CD5⁺ ZAP70⁺   ■ TC⁺CD5⁺
TC⁻ TC⁺

D

TC⁻ ATAμκTg ATA B
CD44
CD24
--- aged non–tumor
— RagKO Thy1KO tumor
— old aged tumor

Breast cancer :
* ECs (epithelial) / MSC
  ECs (endo): **Thy1⁺**
* **Hepcidin⁺**
  – iron deficiency
* EMT- **CD44ʰⁱCD24⁻/low**
* CTNNB1⁺
  HMGB1⁺, Ki67⁺
  CXCR4⁺, serum DPP4⁺

Pancreatic cancer :
* Fibroglasts
  ECs (endo): **Thy1⁺**
* **Hepcidinˡᵒʷ**
  – **iron overload**
* **CD44ʰⁱ** CD24ʰⁱ
  EMT- **CD44ʰⁱCD24⁻**
* CTNNB1⁺ mutation
  HMGB1⁺, Ki67⁺
  CXCR4⁺, DPP4⁺⁺

SARS-CoV-2 :
* ECs / MSC: **Thy1⁺**
* **Hepcidin⁺**
  – iron decreased

SLE:
* MSC: **Thy1⁺**
* **Hepcidin⁺**
  – iron decreased

human Kidney :
* ECs: epithelial cells
  CD90 (Thy1)⁺
* **Hepcidin⁺**
  – iron decreased

human Kidney :
* **CD44⁺** CD24⁺
* CTNNB1⁺ ʰⁱ
  HMGB1⁺, Ki67⁺
  CXCR4⁺, DPP4⁺⁺

* **CD44⁺** CD24⁺
* Urokinase → CTNNB1⁺
  HMGB1⁺, Ki67⁺
  CXCR4⁺, DPP4⁺⁺
* CD5⁺– CD5↓,CD1d↓
  CD22ʰⁱ, CD11b⁺⁺, AID⁺
  CD180⁻, CD21⁻, CD27⁻

E

Hepcidin : **Hamp2**
Microarray Relative mRNA level

FO B | MZ B | sB1a | pB1a | | FO B | **B1a** aPtC V11-2 /Vₖ9 | **B1(a)** ATA B **V8-12** /Vₖ21-5 | **MZ B** AGcA **V8-12** /Vₖ19-17 | **B1(a) ATA B tumor** TCL1 Tg – + ATAμκ Tg
WT (2 mo) | V_H11μTg | ATAμTg | EP67μκTg | ATAμκ Tg (12 mo)

> 16 mo old aged (TCL1 Tg⁻)
ATAμκ (V8-12/ Vₖ21-5) Tg: (n=167)
  ATA B tumor⁺⁺ (CD11b⁺⁺) (46 %)
  ATA B tumor + Myeloid cells⁺⁺ (12 %) (CD11b⁺Gr-1⁺)
AGcA EP67μκ (V8-12/ Vₖ19-17) Tg: (n=41)
  AGcA B tumor (7 %)
  Macrophages⁺⁺ (CD11b⁺Gr-1⁺):
  Spl⁺⁺ (56 %)

22 mo Spl
CD4 / CD8 ; CD11b / 6B2 ; CD11b / Ly6C(Gr-1) 59.5%
→ Intestin/colon tumor⁺⁺ (56 %)

Fig. 5 (See legend on previous page.)

higher in TC$^+$ZAP70$^+$ than TC$^-$. TCL1 leads AKT [113] and mostly AKT2-NF-kB [114]. AKT2 are similar in TC$^-$ to TC$^+$ZAP70$^-$, however, TC$^+$ZAP70$^+$ are increased. Human TCL1 showed higher miR21 and miR155, and lower miR29, and in ATA B cells, these miR showed TC$^+$ > TC$^-$ (Fig. 5B) similar to human TCL1$^+$ CLL [115, 116]. However, down miR15a and miR16 to mediate Bcl2 increase as found in human CLL [117], and similar by down in TC$^-$ than TC$^+$ (Fig. 5B). Low CD21, CD23, CD24, CD27 and CD49d in TC$^-$ ATA B tumor mice are also low in 12 mo TC$^-$CD5$^-$ spl^{++} cells, and these low data can be found in some in U-CLL (CD21, CD27) [94, 99] or low generated (CD23, CD49d) can occur in few CLL [95, 100]. Since normal CD5$^+$ATA B cell and TC$^+$Tg tumor with CD5$^+$ samples are most human TC$^+$ CD5$^+$CLL positive, these in human CLL references also showed in Fig. S4-3. Hamp2^{++}, CD11b^{++} and down CD24 in old aged TC$^-$ ATA B tumor are similar to 12 mo TC$^-$CD5$^-$ cells, but these are not in human CLL.

Increased CD11b^{++}CD22^{++} and Hamp2^{++}

Figure 5C. Originally, B1a cells are CD5$^+$ which bind to SHP-1 as Lyn–CD22–SHP-1. CD22 is from BCR [45], then binding CD5–SHP1 or CD11b–CD22 inhibits BCR signaling [46]. When loss as CD5$^-$ and CD11b$^-$ in spleen B1 [48], middle aged become CD11b$^+$ such as by CpG bacteria or CpG$^+$IL-10$^+$ increase, and in old aged, TC$^-$ ATA B showed increased CD11b^{++}, then increased CD22, and TC$^-$ZAP70$^-$CD5$^-$ are more higher CD11b^{++}CD22^{++} (Fig. 5C). CD22^{++} found in HCL (hairy cell leukemia) [118], however, human CD5$^+$CD11b$^-$CLL is CD22^{lo} not require CD22^{++}, thus different [118]. TC$^-$CD11b^{++}CD22^{++} is allowing the migration and maintaining autoreactive B cell tolerance, and SLE (Systemic lupus erythematosus) found CD11b^{++}CD22^{hi} (Fig. 5D) also autoreactive [46]. α-Thy-1 ATA B cells with CD11b^{++} can Thy-1 moving to endothelial to control virus infection as by CD11b$^+$Gr-1$^+$ endothelial tissues (33.34).

Hamp2 also increased in TC$^-$ ATA B cells in old aged. In hepcidin, mouse ATA B cell tumor did not show Hamp1 but Hamp2^{++}. Hepcidin is important for systemic iron homeostasis, and hepcidin generations are the most CD11b$^+$Gr-1$^+$ macrophage and monocytes, and TLR induced hepcidin in T cells and B cells [42]. Hepcidin control iron is most in liver, however, mouse Hamp2 is in both liver and pancreas with antibacterial and antivirus active types, and B cells including B1 cells can move from spleen to pancreas with high Hamp2 [119], and Hamp2 is not change erythropoiesis different from human hepcidin [120]. In hepcidin, IL-10, IL-6, and IL-22 generate Stat3, then regulate for the induction of hepcidin [121, 122]. In mice, fetal

and neonate showed IL-10 and IL-6 [123, 124]. IL-10 is original B1a cell generation, however, IL-6 did not require for B1a, rather, IL-6$^-$ showed increased B1a cells [125]. Different from Arid3a which is important for neonate mature B1a generation, Arid5a is more adult immature B cell stage and increased IL-6 for B cells [12, 126]. IL-6 reacts with Th2 and Th17, and mostly increased in Th17 [127]. Since in old age, T-bet and CD11c increased [2], T cells changed Th1 and Th17 increase, and Th2 decreased with B cell responsive as IL-4R down (Fig. 5C). High IL-6 in old aged ATA B cell tumor in TC$^-$ZAP70$^-$CD5$^-$ cells are the Arid5a generation with IL-6$^+$ [126] (Fig. 5C) and also IL-10^{++} (Fig. 4A2). Iron regulation require USF2-hepcidin to generate iron [128, 129]. Strongly USF2 high in TC$^-$ cells in ATA B cells (Fig. 5C). In TC$^-$ZAP70$^-$ were high IL-10 and IL-6 than TC$^-$ZAP70$^+$ cells, and higher IL-22 in TC$^-$ZAP70$^+$ in USF2 and IL-22R (Fig. 5C). In Th17 cell, IL-17 and IL-22 generation [130] and TC$^-$ATA B tumor showed highest IL-22 to receptor IL-22R in the highest TC$^-$ZAP70$^+$ cells as Hamp2 highest generation (Fig. 4A2). IL-22 also generated by innate lymphoid cells ILC3 [131]. Cleary, Hamp2^{++} TC$^-$ ATA B tumor cells decreased iron stage, by TFR1$^+$ high (as origin iron) and negative ferroportion FPN (SLC40A1) as iron reduction with TFR1$^+$FPN$^-$ [132]. Thus, old aged TC$^-$ATA B tumor increased Hamp2^{++} and decreased iron (Fig. 5C).

V2-5 human cancers with hepcidin$^+$ or iron$^+$ as mouse V8-12 ATA B1 cell Hamp2$^+$ and AGcA NZ B-macrophage-intestine tumor. V2-5 breast cancer is CD44^{++}CD24^{lo} as old aged ATA B cells

Figure 5D and E. Mouse V8-12 is similar to human V2-5, and HIV-1 virus showed V2-5 and V1-69 generation, and V2-5$^+$ in Ankylosing spondylitis, Alzheimer's disease, and Multiple sclerosis [61–64, 66]. And, human normal kidney present Thy-1$^+$ with V1-69 and V2-5 positive, and several cancers with including V2-5.

Kidney: V3-23, V1-69, V2-5 [133]
Breast cancer: V1-69, V2-5, V3-49, V3-64, V4-59, V5-51 [134]
Pancreatic cancer: high mutatedV3-66, V3-9, V3-38, and low V1-2, V2-5 [135]
SARS-CoV-2(Covid-19): V2-5 or V1-6, V3-53, V2-5 [136, 137]
SLE (Systemic lupus erythematosus): J6 = V2-5, V3-35, V3-33, V7-4, V3-36, V2-26 [138]
In the SLE group, common usage frequencies of the V gene and J gene, and the proportion of IGHJ6 are higher in SLE group

Hayakawa *et al. Immunity & Ageing*   (2024) 21:22

Page 14 of 24

Mouse V8-12 ATA B cells (anti-thymocyte/Thy-1 and polyspecific) are not only CLL, but old aged ATA B cells related to cancer Spl^{++}, mLN^{++}, LN^+, $Liver^{++/+}$.

In human, although T cells are completely absent Thy-1, Thy-1 are present. Thy-1 can move to endothelial stage for tumor suppressor, such as in virus infection, and this Thy-1 move to endothelial cells with dominantly from CD11b in $CD11b^+Gr-1^+$presenting monocytes /macrophase [33, 34] in human. In both human and mice, Thy-1 is in brain neuron together with $CD11b^+$ macrophage [139, 140], thus Thy-1 is important. In human, $Thy-1^+$ is also present in kidney in normal in epithelial cells (ECs) [141], also, urine as a liquid by-product of metabolism generates $hepcidin^+$ [142] (Fig. 5D). As show in Fig. 5D, several cancers also showed $Thy-1^+$ and $hepcidin^+$. In breast cancer, $Thy-1^+$ are present in epithelium ECs together with some MSC (mesencymal stem cells) and in endothelium cells (ECs), and $hepcidin^+$ and iron deficiency [143]. In SARS-CoV-2, epithelium ECs and MSC with $Thy-1^+$, and $hepcidin^+$ with iron decreased [144]. In SLE, most MSC are CD90 (Thy-1), CD105, CD73 positive, and $hepcidin^+$ and iron decreased [145]. Human pancreas is different from mouse in $Hamp2^+$ in pacreas [119], and in human pancreatic cancer, fibroblasts and endothelium ECs present Thy-1, however, hepcidin low and iron overload [146], with high macrophage and neutrophil interaction in pancreatic tumor microevironment [147], not normal increases hepcidin. Thus, pancreatic cancer is the different paper to generate high macrophage with low hepcidin and iron overload.

CD44 is homing receptor and original pB1a are higher than FO B cells (Fig. S2B), and more increased in old aged ATA B tumor. CD24 (30F1) is a glycophosphatidylinositol (GP1)-anchored protein, with all normal B cells express. CD24 overexpressed in tumor and human CLL [96], and mature & middle ATA B tumor under Rag1KOThy1KO mice showed also higher CD24, then, old aged ATA B tumor showed down CD24 (Fig. 5D). $CD44^{hi}CD24^{-/low}$ are well known for human breast cancer [148], originally generated by EMT (epithelial-mesenchymal-transiton) [149]. EMT plays a key role in the regulation of cell motility and invation. In pancreatic cancer, $CD44^{hi}CD24^{hi}$, but when non-B cell EMT presented $CD44^{hi}CD24^-$ [150]. DAMP/HMGB1 can present EMT [151], and AID also increased EMT [152]. Since old aged ATA B tumor showed DAMP/$HMGB1^+$ and AID^+, it is possible that EMP increased with changed to $CD24^{low}$ with $CD44^{++}$. Ki67 is increased from HMGB1 [153], and TC^-ZAP70^+ showed both highest Ki67 and HMGB1, then lowest CD24 in TC^-ZAP70^+ than TC^-ZAP70^- (Fig. 4A3). However, also, $p16^{INK4A}$ reduction increase EMT [154], and C.B17 mice are $p16^{INK4A}$ mutation and human breast cancer are often $p16^{INK4A}$ mutation (49%)

[155], thus, ATA B $CD24^{low}$ with EMT may be the more generated incruding by $p16^{INK4A}$ reduction in old age.

Similar to old aged mouse ATA B tumor, human breast cancer showed $CXNNB1^+$, $HMGB1^+$, $Ki67^+$, $CXCR4^+$ and serum $DPP4^+$. Pancreatic cancer showed $CTNNB1^+$mutation, $HMGB1^+$, $Ki67^+$, $CXCR4^+$, $DPP4^+$. SARS-CoV-2 showed, $CTNNB1^{hi}$, and serum $HMGB1^{hi}$ and dominant T cells showed $Ki67^+$, and $CXCR4^+$, $DPP4^{++}$. In SLE, CTNNB1 low but urokinase-type plasminogen activator made $CTNNB1^+$, and serum $HMGB1^+$, and $Ki67^+$, $CXCR4^+$, $DPP4^+$. Then, SLE originally known by presented $CD5^+$ B cells, then, CD5 decreased B cells can occurred, also CD1d downregulated. As found in mouse old aged ATA B tumor, SLE are known the autoimmune disease and generated $CD5^-$, $CD1d^-$, $CD22^{hi}$, $CD11b^{++}$, AID^+, $CD180^-$, $CD21^-$, $CD27^-$ (Fig. 5D), also T-bet^{hi} $CD11c^{hi}$ and $TCR7^+$ $TCR9^+$. All reference in Fig. 5D listed in Fig. S5: Brest cancer, Pancreatic cancer, SARS-CoV-2, and SLE.

Figure 5E. B cells can cross talk fibroblast and became to epithelial cells [156], and B-1 B1 B cells and B-2 MZ B cells interacts macrophage and dendritic cells [157, 158], and the spleen MZ B cells clearly contains macrophage receptor. As human CLL showed some increased myeloid cells, old aged mouse ATA B tumor showed increased $CD11b^+Gr-1^+$ myeloid cells/macrophage with 12% (Fig. 5E) [13]. V8-12 μTg cells showed increased in MZ B with V_k19-17 as AGcA, and generated V8-12/V_k19-17μκTg mice strongly AGcA MZ B cell generation at first 3 wk as early B-2 stage [54] (Fig. S3), and this AGcA MZ B cells showed increased Hamp2 at 12 mo, as ATA B1 cells $Hamp2^+$, however V11-2 aPtC B1a cells are not increased Hamp2 (Fig. 5E). In old aged, originally AGcA MZ B cells can become tumor 7%, but macrophage with $CD11b^+Gr-1^+$ are most strongly increased in spleen by MZ B cells as $spleen^{++}$ (56%), and high intestine/colon tumor generated (Fig. 5E, and pictures in Fig. S3), also resulting in a upper respiratory swollen neck (Fig. S3). Human HIV-2 virus are V2-5 positive [61] and accumulated macrophage and hepcidin increases with iron decrease, thus maintenance of viral set-point [159, 160]. Ankylosing spondylitis (AS) with most V_H2 (dominant V2-5) [62] are the neutrophils progression, and Alzheimer's disease in brain (AD) found in V2-5 are with macrophage polarization subsets, most in bacteria [161]. Both AS and AD showed $hepcidin^+$ plays with an important role [162, 163]. Multiple sclerosis (MS), also V_H2 (dominant V2-5) positive [66], as a brain-gut axis and blood–brain, with important macrophage [164], however, with low hepcidin and crucial role of iron in serum [165]. Clearly, increased iron in brain in MS in age [163], and MS is intestinal barrier occur with iron [166, 167]. Aging spleen macrophage can increase tumor-derived

Hayakawa *et al. Immunity & Ageing*   (2024) 21:22

Page 15 of 24

factor with iron$^+$ in mice [168] and macrophage-iron$^+$ in old/damaged generate red blood cells, generate brain functions (brain-spleen axis) and generated colon (spleen-gut axis), then gut-brain-spleen axis [166]. These iron$^+$ in tumor generation in human is TFR1^{hi} and FPN$^+$, not FPN^{lo} [169]. Human V2-5$^+$ cancer with macrophage/neutrophils generate mostly high hepcidin with iron deficiency, however, pancreatic cancer and multiple sclerosis (MS) are macrophage generate with high iron with low hepcidin, similar to mouse V8-12$^+$ AGcA MZ B increased macrophage to generate intestinal/colon tumor. Clearly, human V2-5 homologous to mouse V8-12. Mouse old age ATA B cells showed CD11b^{++} with control Thy-1 and directly Hamp2^{++} and some increased macrophage, and MZ B showed strongly macrophage increased in spleen with tumor-derived factor.

IgVH in TC$^+$Tg lymphoma/leukemia

TC$^+$Tg ATA B cells are different from TC$^-$ old aged tumor. We previously published TC$^+$Tg generated tumor and found most VHs are as B-1 cell CLL tumor [24] (Fig. 6). In this TC$^+$Tg C.B17 mice, generation of ATA B cells were low (than SM/J and NZB mice), rather, showed several increased IgV$_H$. Dominantly high in J558 (V1-55, V1-52), V$_H$12 anti-PtC (V12-3), Q52 anti-MyIIA (V2-9). In J558 V1 cells, TC$^+$Tg generation (V1-55, V1-52, V1-82, V1-9, V1-19, V1-78), and in normal C57BL/6 B1a cells V1-55 and V1-53 are high beginning at 2-3wk [170], and V1-14 as anti-Sm for B1a cell. All these V1 showed slightly increased level in human V1-46. Human CLL is low V1-46, however, ratavirus-specific B cells showed high V1-46 [171], and, when repertoire of rotavirus generation, young children showed highest V1-46 [172].

V$_H$12 (V12-3), Q52 (V2-9, V2-2), 36–60 (V3-2, V3-8, V3-6) showed slightly reacted to human V4-59 (lower V6 than V4-59). In both cord blood and adult blood in human, V1-69 and V4-59 are the higher list, and in cord blood with depth analysis, V4-59 > V4-43 > V2-5 [173]. Also, in older subjects, V4-59 is also positive. In human CLL, V4-59 is the medial level with mutated or some non-mutated [174]. V4-59 also occurred in HCL (hepatitis C virus) [175], and MCL (mantle cell lymphoma) showed V3-21(mutant) and V4-59 (not/low mutate) [176].

S107 (V7-3, V7-1) are positive with human V3-49, V$_H$11 (V11-2) is positive with V3-74, J606 (V6-4) and X24 (V4-1) are positive with V3-7, and 7183 (V5-17, V5-9, V5-12, V5-6) showed different V3 positive. In human CLL, V3-7 and V3-23 are positive (V3-7 are mostly mutant, and V3-23 are low mutant or mutant), and V3-49, V3-21, V3-74 are low in CLL [174]. Mouse aPtC V11-2 are well known for mouse B1a cells, and human V3-74 showed high in celiac disease (CeD)-specific antibodies in gut (gastrointestinal tract), and human aPC showed V3-74 [177]. Since mouse V1-55 and V1-52 (similar to human V1-46), and V12-3 and V2-9 (similar to human V4-59) were higher in TC$^+$Tg cells, we next checked the region for higher these V$_H$ cells in TC$^+$ Tg B-1 tumor cells.

High increased B-1 VH cells generated in TC$^+$Tg are not only related to fetal/neonatal generation

As shown in Fig. 7A, neonate liver HSC (hepatic stellate cells) generate myeloid progenitor (CMP) and lymphoid progenitor (CLP). Innate immune system in CMP generate myeloblast (GMP) and erythrocyte and megakaryocytes-platelets generation (MEP). In CLP, B-1 cells generated under Lin28b$^+$Let7$^-$ and Arid3a$^+$ allowed generation of CD5$^+$ B1a cells. Several B1a binds to erythrocyte under aPtC (phosphatidyleholine): V$_H$11 (V11-2), V$_H$12 (V12-3), J558 (V1-53), and aMyIIA (non-muscle myosin IIA) Q52 (V2-9) also can bind to erythrocytes and platelets. These B1a binding to erythrold cells are high in neonate than adult stage [43] (Fig. 7A). In TC$^-$ aged, aPtC (V11-2, V12-3, V1-53) and aMyIIA (V2-9) showed lymphoma [25, 178], and in old aged V11-2 μTg mice (V$_H$11t) generated MBC (monoclonal B cell lymphocytosis) in PBL [13], and aMyIIAμκTg (as ON25) generated aMyIIA B CLL/lymphoma [25] (and Fig. S1C). Since human V1-67 and other IgH in U-CLL can bind to MyIIA [179], mouse neonate TC$^-$aMyIIA B cell became similar to human TC$^+$U-CLL. J558 (V1-52) reacted for E-coli from early B1a cells, also generation of lymphoma. J558 (V1-55) is not found in earliest neonate stage, then, at 2–3 wk high increased in C57BL/6 mice [170], and when LPS$^+$ generation, strongly CLL/lymphoma generation occur by V1-55 in age in C.B20 mice [180]. In TC$^+$ Tg in C.B17 mice, highest V12-3 and V1-55, and higher V2-9 and V1-52 in CLL [24].

Erythrold cells are lower in 2 mo than neonate stage [43] (Fig. 7A). Originally Lin28b$^+$ in neonate generated B1a V$_H$11 and V$_H$12 are continuously incrused in 2 mo Lin28b$^-$ Spl and PerC. In contrast, when Lin28b$^+$ Tg generate, V1-55 became highest in 2 mo adult, contrast downregulate V$_H$12 and V$_H$11 [43] (Fig. 7A). In adult BM, pro-B to pre-B cell generation requires TdT (Terminal deoxynucleatidyl transferanse) for N-necleotides to the V.D. and Jexon of the BCR, in contrast, N-region can not require in fetal and neonate [181]. TdT decrease as TdT KO mice together with Lin 28b$^+$ Tg mice showed negative in V1-55, contrast, increased in several earliest generated B1 related cells such as V$_H$11 and Q52 (V2-9), although not increased in V12-3. When B-1 pro- to pre-B cell stage by binding to surrogate light chain (SLC) associated in B-2 stage, clearly that V11-2, V2-9, V1-52 are negative, and middle by V8-12, then positive by V1-55 and V12-3, as previously identified [24]. Thus, B-1 V12-3 and V1-55

Mouse Eμ-TCL1 Tg⁺ B-Lymphoma / Leukemia IgVH

Mouse V$_H$ gene		Human V$_H$ gene subgroup					C.B17 mice TC⁺ CLL tumor total n= 148
		V1-46	V1-2	V1-3	V1-18	V1-69	n=
J558	V1-55	**70.4**	69.4	69.4	68.4	67.3	20
	V1-52	**68.4**	65.3	66.3	61.2	63.3	10
	V1-82	**66.3**	64.3	65.3	62.2	65.3	4
	V1-9	**67.3**	**67.3**	64.3	63.3	66.3	3
	V1-19	**68.4**	67.3	67.3	64.3	62.2	3
	V1-78	**64.3**	62.2	63.3	61.2	62.2	3
	V1-53	**71.4**	69.4	69.4	65.3	63.3	–
	V1-14	**70.4**	69.4	**70.4**	66.3	66.3	–
		V4-59	V4-31	V4-61	V4-39	V4-34	
VH12	V12-3	**68**	67.7	65.6	63.6	61.8	39
Q52	V2-9	**66.6**	62.6	63.6	62.6	52.7	16
	V2-2	**59.8**	59.6	59.6	56.6	52.6	4
36-60	V3-2	**74**	73	72.9	71	65.6	4
	V3-8	**71.1**	68.7	66.7	62.6	61.8	3
	V3-6	**74.2**	72.7	72.7	69.7	67	2

Mouse V$_H$ gene		V3-7	V3-49	V3-23	V3-21	V3-30	V3-74	n=
S107	V7-3	71.4	**79**	72.4	69.4	68.3	72.4	5
	V7-1	69.4	**73**	70.4	65.3	66.3	68.4	2
VH11	V11-2	65.3	60	64.3	64.3	63.3	**67.3**	4
J606	V6-4	**73.5**	72	72.4	70.4	71.4	72.4	2
X24	V4-1	**69.4**	56	66.3	66.3	64.3	66.3	2
7183	V5-17	79.6	66	79.6	**83.6**	79.6	79.6	2
	V5-9-1	73.5	64.7	**75.5**	75.5	73.5	71.4	2
	V5-12	74.5	65.3	**76.5**	75.5	71.4	74.5	1
	V5-6	**80.6**	68	79.6	79.6	77.5	79.6	1

> 6% TCL1 Tg⁺ tumor, **B-1 B cells**:　　　　　　　　　　anti -

(26.4%): V12-3 (VH12, VH12-01, V261)- D-JH1 /V$_k$4-91　– PtC

(13.5%)- V1-55 (J558-64, V332: 165.1)-D-JH1,4 / V$_k$12-89– idiotype
　　　　　　　　　　　　　　　　　　　　　　　　　　dsDNA

(10.8%): V2-9 (Q52-1, V222:　Ox-1) -D-JH4　/ V$_k$9-96 – MyIIA

(6.7%): V1-52 (J558-67, V328: CH31)-D-JH1　/ V$_k$1-117 – E-coli

Mouse TCL1 Tg⁺ B cell tumor V$_H$
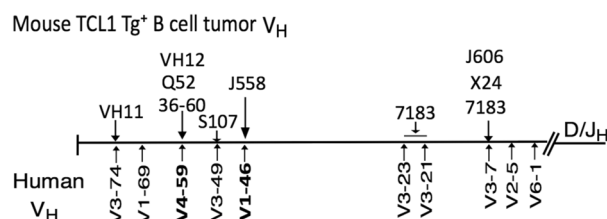
Fig. 6 Mouse TC⁺Tg B-lymphoma/leukemia IgVH list. TC⁺Tg C.B17 mice generated CLL tumors were previously published [24], then, found mouse V1 generated tumor is slightly similar with human V1-46, and mouse V12, V2, and V3 generated tumor are similar with human V4-59. Mouse V7, V11, V6, V4, V5 generated tumors are each different in human V3. Higher TC⁺Tg tumors (V1-55, V1-52, V12-3, V2-9) are with mouse non-mutated B-1 B cell origin

can continue to generate to B-2 immature B cells not only early B-1 stage, then, TC$^+$Tg aloud increased. Anti-PtC V$_H$11 and V$_H$12 are different. Both react with BrMRBC (bromelain-treated mouse erythrocyte), however, V$_H$11 as a stage of TMA(trimethylammonum) present, and anti-TMA response reflects the V$_H$11 usage in original mice [182], in contrast, V$_H$12 showed high reaction with SRBC(sheep red blood cells) as sheep erythorocytes with continuously increase [182]. Since TC$^+$Tg mice continuous generate TC$^+$, more generated in V12-3 and V1-55 in age, but, early strongly neonate stage V2-9 (aMyIIA) and V1-52 can also increased in age (Fig. 7A).

In neonate ATA B cells, TC$^+$Tg ATAμκTg ATA B mice showed continuously slightly higher Let-7 as adult Lin28$^-$Let7$^+$ than TC$^-$, thus, TC$^+$Tg changed. TC$^-$ATA B cells showed lower miR150 and miR181b than TC$^+$Tg (Fig. 7B). miR150 and miR181b are originally low in neonate B1 cells since Lin28$^+$ downregulate miR150 and miR181 [183, 184], and well known that original miR150$^-$ makes in human B1a cells [185], and human U-CLL are miR150^{low} [186]. In adult miR181 are positive, then, TC$^+$ human old aged, miR181 can be decreased, and showed miR181b^{low} is making progression and cell death resistance with human cancer, and miR181 down regulation showed increase TCL1 in human [187]. Thus, old aged mouse TC$^-$ ATA B tumor with down miR181b similar to human CLL progression [188], without increased TCL1 in mice. TC$^-$ ATAμκTg tumor showed increased CD11b and Hamp2 in middle aged CLL, and further increased in old aged, different from TC$^+$Tg. (Fig. 7C).

Old aged TC$^-$ ATA B cell lymphoma/leukemia with old aged human CLL/U-CLL, and increased Hamp2 as in human cancer hepcidin$^+$

Summarized in Fig. 7D. TCL1 are positive in embryo, originally. Then, in mice, TCL1 (as TCL1A) down regulated at 18 day in fetal liver as TC$^-$ [16], thus, TC$^+$Tg generation showed continuously TC$^+$ fetal/neonate and aged. Originally generated B1 cells in TC$^+$Tg are sertein IgH cells increased in CLL Lynphoma/Leukemia at middle aged with increased NF-kB in reaction to bacteria or viruses generated. Middle age TC$^+$Tg mice tumors are not all similar to old aged. In TC$^-$B1a cells at neonate-early age stage, mature IgH cell levels are different from mouse background, then, certain original TC$^-$B1a cells VHs can generate in old age lymphoma/leukemia. In old aged, both mouse and human generate more T-bet$^+$CD11c$^+$ as different T cells, and increased myeloid cell differentiation [189]. Then, increased TCL1 in human CD5$^+$B cells can occur with sensitive bacteria increase generating CLL. Since CD5$^+$ cells leads to stop of BCR signaling, ZAP70$^+$ further required for immediate strongly in human TC$^+$ZAP70$^+$CD5$^+$ U-CLL for more aggressive with a significantly short time than M-CLL. In mice, increased ZAP70 can several increase than ZAP70$^-$, but CD5 down with high CD11b^{++}CD22^{++} in TC$^-$ZAP70$^-$CD5$^-$ can also occurred lymphoma/leukemia generation in old age, and high Hamp2^{++}.

In ATAμκTg mice in neonate and early aged, B1a cells increased Nod1$^+$, IL5R$^+$, CD1d$^+$, CTLA4$^+$, CXCR5$^+$ (in pB1a^{hi}), cyclin D2$^+$, cMyC$^+$, and CD11b$^+$ in pB1a (not sB1a), as also normal B1a cells. Since C.B17 mice has p16^{INK4a} mutation, further high cyclin D2. In old aged ATA B cells, decreased originally Nod1, IL-5R, CD1d, CTLA4, CXCR5, also CD49d in B1a cells. In contrast, cyclin D2, cMyc, also CD38, CD44, CD43, STAT3, BAFF, were more increased in old aged and CD11b increased. And, high T-bet$^+$CD11c$^+$ and miR181b^{low} in old aged are similar to human old aged CLL. In old aged TC$^-$ATA B mice, ZAP70$^-$CD5$^-$ and ZAP70$^+$CD5$^+$(also CD5$^-$), are generated with increased cells or down cells similar to human CLL/U-CLL (Fig. 7D). Different from human CLL, ATA B cells showed often CD5 down by bacteria in aged, then with increased CD11b^{++}CD22^{++} by highest in old age, and the Hamp2^{++} with decreased iron. Decreased CD24 in mouse old aged ATA B tumor cells by including from p16^{INK4a} mutated. Human several cancers showed hepcidin$^+$ with decreased iron, and hepcidin$^+$ increased by CD11b$^+$Gr-1$^+$ macrophages/neutrophils. Mouse old aged V$_H$8-12/V$_k$21-5 ATA B cells generated directly high Hamp2 and iron decrease in B1 cells. Different to ATA B1 cells, mouse V$_H$8-12/V$_k$19-17 AGcA

(See figure on next page.)
Fig. 7 TC$^+$Tg B1 B cells in neonate to early age are changed than TC$^-$. Old aged TC$^-$ATA B cells similar to human CLL/U-CLL and further some different. **A** Summary. In B-1 B cell generations, aged ability for lymphoma or CLL/lymphoma [13, 25, 178, 180], and V1-55 in C57BL/6 mice is high at 2-3 wk, than 1 wk [170]. Down: 2 mo Lin28 Tg$^+$ changed are high V1-55 and decreased V1-55 with negative TdT^{KO} Lin28 Tg$^+$ persentage, as TdT requaded for B-2 from Pro-B (TdT$^+$) move to Pre-B. When V1-55 and V12-3 B-1 Pro-B to Pre-B cell stage with heavy chain with surrogate light chain (SLC) association to B-2 analysis. Thus, increased in TC$^+$Tg. **B** 12 mo microarray relative miRNA level Let-7 showed slightly higher in TC$^+$Tg ATA B cells than TC$^-$, and TC$^-$ ATA B are low miR150 and miR181b. **C** High increased CD11b and Hamp2 in old age TC$^-$ ATAμκTg mice. **D** Conclusion of difference of TC$^+$Tg and TC$^-$ mice to generated lymphoma/leukemia, and in C.B17 mice TC$^-$ATAμκTg ATA B from neonate, middle age, and old aged. Old age ATAB lymphoma/leukemia generation with most similar to human TC$^+$CLL/U–CLL and different to CLL with CD11b^{++}Hamp2^{++}, CD22^{++}, CD24$^{lo/-}$. CD23$^-$CD49d^{low} are the some generated cancers. AGcA generate MZ B and changed to increased macrophages^{++} with intestine/colon tumor in old age
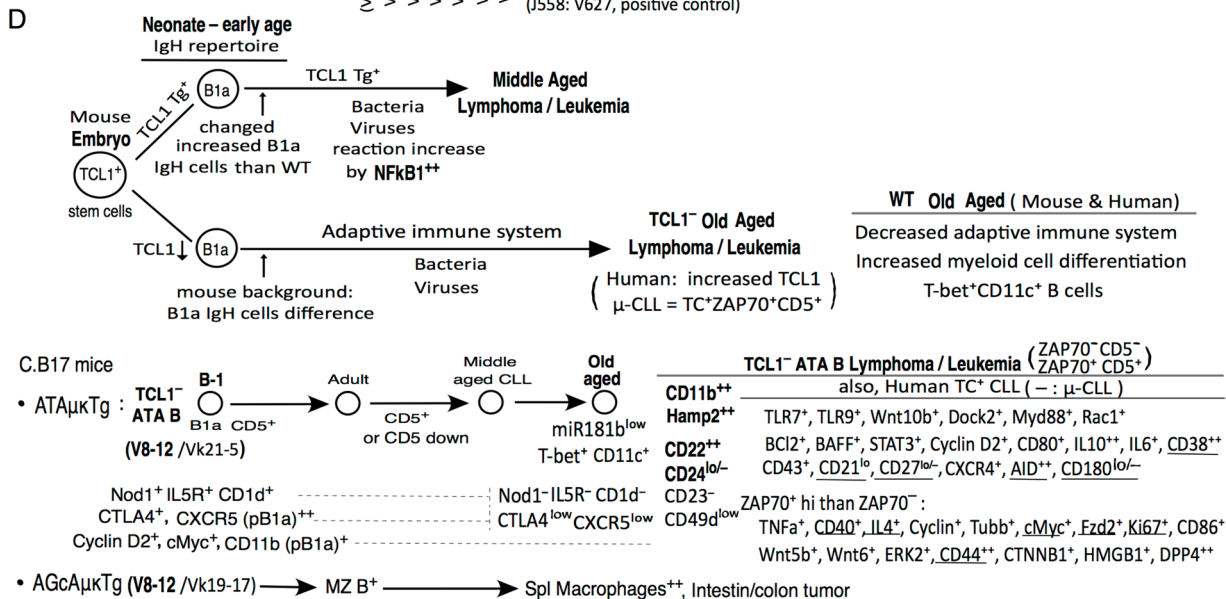
Fig. 7 (See legend on previous page.)

Hayakawa *et al. Immunity & Ageing*   (2024) 21:22

Page 19 of 24
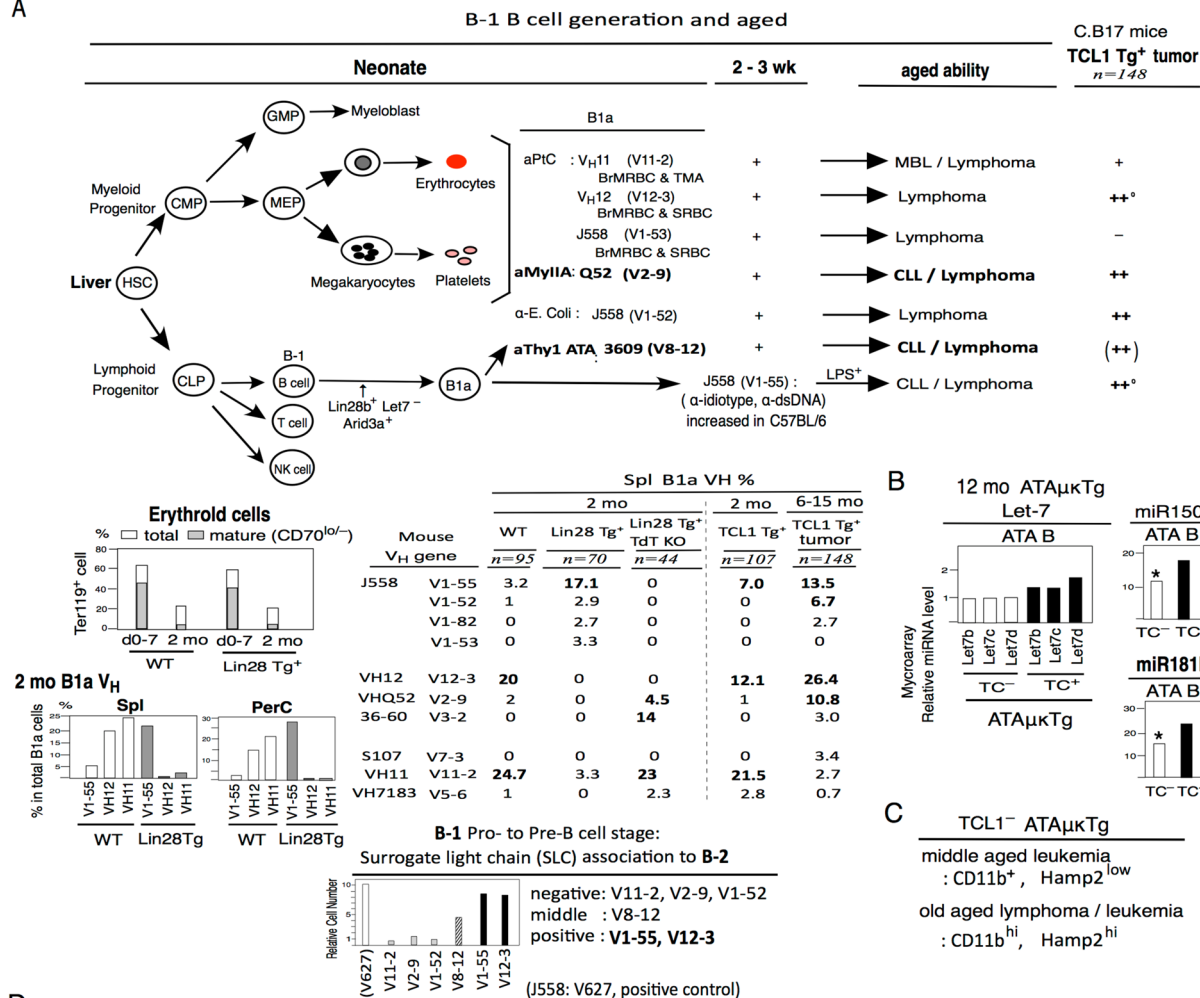
generate MZ B cells increased high macrophage, then, intestine/colon tumor generation.

Conclusion

Neonate V_H8-12/V_k21-5 CD5$^+$ATA B cells generated old aged leukemia/lymphoma without TCL1. ATA B cells can decrease CD5 in middle age and increase CD11b^{++}CD22^{++} in ZAP70$^-$CD5$^-$, generating old age leukemia/lymphoma with autoimmune disease and control Thy-1, also ZAP70$^+$CD5$^+$ with CD11b$^+$CD22$^+$. This mouse TC$^-$ATA B cell tumors in old age most similar to human old age TC$^+$ CLL/U-CLL, and middle aged TC$^+$Tg ATA B mouse tumors are not similar to old aged in TC$^-$ mice, but increased ZAP70$^+$ made several increased data as in old aged TC$^-$. Certain original generated in mouse B1 cell genes decrease or increase in old age. Then, ATA B cells are hepcidin-related Hamp2 increased with iron^{low} as similar to human cancer hepcidin$^+$ iron^{low}. Mouse V8-12 similar to human V2-5, and V2-5 related to several cancers with hepcidin$^+$iron^{low} generated macrophage/neutrophils, and multiple sclerosis are hepcidin$^-$iron$^+$ generated from macrophage including brain-gut/colon axis. Mouse V_H8-12/V_k19-17 generate AGcA MZ B cells increased macrophage with intestine/colon axis tumor with old age. Conclusion, mouse with V8-12 in old aged, B-1 cells generated CLL/cancer and B-1 cells directly with Hamp2^{++} Iron^{low}, contrast, B-2 MZ B cells increased macrophage in spleen with intestinal/colon tumor. Since V_H8-12/V_k2-5 B1cells can also interacts macrophages, mouse V8-12 similar to human V2-5 generated macrophage/neutrophil with hepcidin$^+$iron^{lo} or hepsicin$^-$ iron$^+$.

Materials and methods

C.B17 mice is the BALB/c background with changed as IgM^b. Originally generated anti-thymocyte/Thy-1 (ATA) B cells (IgM^a) in SM/J mice [10], and generating ATAμκTg and ATAμTg under C.B17 mice with ATA B lymphoma/leukemia generation in old age [10, 11, 24]. Thy-1KO or Rag1KO under ATAμκTg were generated [55], and ATAμTg generated MZ B cells as AGcA B cells and AGcAμκTg generated dominant MZ B cells were published [54], and continuously analyzed for AGcAμkTg mice in old age, with high macrophage in spleen and generated in intestinal tumor. Eμ-TCL1 transgenic mice (TC$^+$Tg) in C.B17 mice, also with ATAμκTg or ATAμTg, and showed generated lymphoma/leukemia [24]. In this paper, microarray gene-expression analysis of ATA B lymphoma/leukemia by old age TC$^-$ versus middle age TC$^+$Tg in ATAμκTg tumor and 12 mo TC$^-$CD5 down ATAμκTg comparison.

Microarray gene-expression analysis

mRNA expression analysis using Agilent Technologies whole genome arrays**.** Total RNA, isolated as described previously [190], was used for production of fluorescent-labeled probe and then hybridized to the array. RNA purity and integrity were evaluated using the 2100 Bioanalyzer (Agilent Technologies) and NanoDrop 1000 (Thermo Fisher Scienti c) before probe generation. Experimental samples were labeled with either Cy3 or Cy5, and a common reference RNA, a pool of total RNAs from several mouse organs generated in the laboratory, was also fluorescent labeled. Each sample was done twice with dye-swap as technical replicates. Hybridized slides were scanned on an Agilent Technologies scanner, and fluorescent intensities of hybridization signals were extracted using Agilent Technologies Feature Extraction software. Statistical analysis was performed in the Fox Chase Biostatistics Facility.

miRNA expression analysis. Total RNA was isolated using TRIzol reagent (Invitrogen) and washed with 80% ethanol to better retain small RNAs. The RNA quality and integrity were evaluated using the 2100 Bioanalyzer and NanoDrop 1000. 100 ng total RNA was dephosphorylated with calf intestinal phosphatase and then end-labeled with Cyanine-3-pCp using T4 RNA ligase. Labeled RNA was hybridized to the Agilent Technologies mouse miRNA microarray at 55 °C for 20 h. Slides were washed according to the Agilent Technologies miRNA protocol and scanned. Signals were extracted as described above.

Flow cytometry analysis

Flow cytometry analysis, sorting and monoclonal antibody reagents, including CD11b (M1/70), CD40 (1C10), CD80 (16-10A1), CD86 (GL-1), CD38 [90], CD43 (S7), CD44 (IM7), CD21 (7G6), CD23 (B3B4), CD24 (30F1), CD27 (LG.3A10), CD49d (R1-2), Gr-1(RB6-8C5). Nod1$^{-/-}$ mice were originally made [68], and generated in 4 mo ATAμκTg Nod1$^{+/-}$ and Nod$^{-/-}$ under C.B17 mice. Animal experiments were conducted under a protocol approved by the FCCC Institutional Animal Care and Use Committee (IACUC).

Quantitative RT-PCR assay

Gene expression was quantitated by real-time PCR, using TaqMan assays from Applied Biosystems, an ABI 7500 real-time thermal cycler, and ABI software (Life Technologies). Relative gene expression levels were normalized using β-actin values for mRNA as a standard.

For spleen FO B versus pB1a in 2 mo, check of increased ZAP70 by anti-IgM, TNFa (aa80-235), DAP (C12-iE-DAP) (from InvivoGen), MDP (from

Hayakawa *et al. Immunity & Ageing*　　(2024) 21:22

Page 20 of 24

InvivoGene). FO B (1×10^5, 25λ) and pB1a cells (1×10^5, 25λ) and together with anti-mouse IgM (15λ), DAP(15λ), MDP(15λ), TNFa (100 ng/ml, 15λ), then 20 h later, RT-PCR analysis with ZAP70.

Intestinal microbiota

This intestinal microbiota positive analysis was published [25]. Crossreactivity of ATA IgM with intestinal microbiota as small intestine and large intestine as colon. For microbiota staining, fecal microbiota were prepared from C.B17.*scid* mouse intestine and incubated with 2 ug/ml IgM at room temperature for 60 min, followed by FL-anti IgM at 4 °C for 20 min, and then analyzed by flow cytometry. Monoclonal IgM (anti-KLH MM-30, BioLegend) was also used as a control.

Heavy chain with surrogate light chain (SLC) association analysis

This was published for aMyIIA as negative and control IgH (SP6, V627) [25]. *IgH retrovirus production*: Selected IgH VDJ segments were amplified by PCR, cloned into an IgH-μ construct, and inserted into the pMIG retroviral vector (MSCV-IRES-GFP). Each IgH-pMIG plasmid and the pCL-Eco retroviral packaging vector were co-transfected into the Phoenix packing line and 24 h supernatant was collected, filtered, and stored at -80 °C until use. To analyze *Ig heavy chain associated with SLC (examine surrogate light-chain)*: Pro-B Abelson line N38 was transduced with IgH-pMIG retroviral supernatant. In GFP$^+$ (green fluorescent protein) cells, IgH-μ transduction was examined by intracellular IgM staining, and extent of SLC assembly was examined by surface SLC staining, using the conformation-dependent anti-surrogate light-chain antibody SL156. To test the capacity for pre-BCR-mediated proliferation, IgH-pMIG retroviral supernatant was added to pro-B cell sultures of Rag1$^{-/-}$ BALB/c BM on OP9 stromal cells together with IL-7. IgH (SP6, V627) as a positive control was set to 10.

Supplementary Information

The online version contains supplementary material available at https://doi.org/10.1186/s12979-024-00415-6.

Additional file 1: Figure S1. Summary. In age, ATA B increased in PBL and CD5 can decrease, and increase of CD11b in ATA B, aMyIIA, and aPtC. V8-12 generation in MZ B cell.

Additional file 2: Figure S2. 2 mo wild time (WT) B1a cells versus ATAμκ Tg ATA B tumor.

Additional file 3: Figure S3. AGcA generation of NZ B and old aged generation of macrophages++ and intestinal tumor.

Additional file 4.

Additional file 5.

References

1. Shyh-Chang N, Daley GQ. Lin28: primal regulator of growth and metabolism in stem cells. Cell Stem Cell. 2013;12:395–406.
2. Rubtsova K, Rubtsov AV, Cancro MP, Marrack P. Age-Associated B Cells: A T-bet-Dependent Effector with Roles in Protective and Pathogenic Immunity. J Immunol. 2015;195:1933–7.
3. Hamblin TJ, Davis Z, Gardiner A, et al. Unmutated Ig V(H) genes are associated with amore aggressive form of chronic lymphocytic leukemia. Blood. 1999;94:1848–54.
4. Damle RN, Wasil T, Fais F, et al. Ig V gene mutation status and CD38 expression as novel prognostic indicators in chronic lymphocytic leukemia. Blood. 1999;94:1840–7.
5. Prabakaran P, Chen W, Singarayan MG, et al. Expressed antibody repertoires in human cord blood cells: 454 sequencing and IMGT/HighV-QUEST analysis of germline gene usage, junctional diversity, and somatic mutations. Immunogenetics. 2012;64:337–50.
6. Amato T, Sall A, Dieye TN, et al. Preferential Usage of Specific Immunoglobulin Heavy Chain Variable Region Genes With Unmutated Profile and Advanced Stage at Presentation Are Common Features in Patients With Chronic Lymphocytic Leukemia From Senegal. Am J Clin Pathol. 2017;148:545–54.
7. Ma S, Shukla V, Fang L, et al. Accelerated development of chronic lymphocytic leukemia in New Zealand Black mice expressing a low level of interferon regulatory factor 4. J Biol Chem. 2013;288:26430–40.
8. Phillips JA, Mehta K, Fernandez C, Raveche ES. The NZB mouse as a model for chronic lymphocytic leukemia. Cancer Res. 1992;52:437–43.
9. Eisenberg RA, Theofilopoulos AN, Andrews BS, et al. Natural thymocytotoxic autoantibodies in autoimmune and normal mice. J Immunol. 1979;122:2272–8.
10. Hayakawa K, Carmack CE, Hyman R, Hardy RR. Natural autoantibodies to thymocytes: origin, VH genes, fine specificities, and the role of Thy-1 glycoprotein. J Exp Med. 1990;172:869–78.
11. Hayakawa K, Asano M, Shinton SA, et al. Positive selection of anti-thy-1 autoreactive B-1 cells and natural serum autoantibody production independent from bone marrow B cell development. J Exp Med. 2003;197:87–99.
12. Shinton SA, Brill-Dashoff J, Hayakawa K. Pla2g2a promotes innate Th2-type immunity lymphocytes to increase B1a cells. Sci Rep. 2022;12:14899.
13. Hayakawa K, Formica AM, Nakao Y, Ichikawa D, et al. Early Generated B-1-Derived B Cells Have the Capacity To Progress To Become

Hayakawa *et al. Immunity & Ageing*   (2024) 21:22

Page 21 of 24

Mantle Cell Lymphoma-like Neoplasia in Aged Mice. J Immunol. 2018;201:804–13.

14. Hallas C, Pekarsky Y, Itoyama T, et al. Genomic analysis of human and mouse TCL1 loci reveals a complex of tightly clustered genes. Proc Natl Acad Sci U S A. 1999;96:14418–23.

15. Narducci MG, Fiorenza MT, Kang SM, et al. TCL1 participates in early embryonic development and is overexpressed in human seminomas. Proc Natl Acad Sci U S A. 2002;99:11712–7.

16. Narducci MG, Virgilio L, Engiles JB, et al. The murine Tcl1 oncogene: embryonic and lymphoid cell expression. Oncogene. 1997;15:919–26.

17. Weng J, Rawal S, Chu F, et al. TCL1: a shared tumor-associated antigen for immunotherapy against B-cell lymphomas. Blood. 2012;120:1613–23.

18. Kipps TJ, Robbins BA, Carson DA. Uniform high frequency expression of autoantibody- associated crossreactive idiotypes in the primary B cell follicles of human fetal spleen. J Exp Med. 1990;171:189–96.

19. phenotypic and functional studies. Antin JH, Emerson SG, Martin P, et al. Leu-1+ (CD5+) B cells. A major lymphoid subpopulation in human fetal spleen. J Immunol. 1986;136:505–10.

20. Bondada S, Bikah G, Robertson DA, Sen G. Role of CD5 in growth regulation of B-1 cells. Curr Top Microbiol Immunol. 2000;252:141–9.

21. Sen G, Bikah G, Venkataraman C, Bondada S. Negative regulation of antigen receptor- mediated signaling by constitutive association of CD5 with the SHP-1 protein tyrosine phosphatase in B-1 B cells. Eur J Immunol. 1999;29:3319–28.

22. Herling M, Patel KA, Weit N, et al. High TCL1 levels are a marker of B-cell receptor pathway responsiveness and adverse outcome in chronic lymphocytic leukemia. Blood. 2009;114:4675–86.

23. Chen L, Widhopf G, Huynh L, et al. Expression of ZAP-70 is associated with increased B- cell receptor signaling in chronic lymphocytic leukemia. Blood. 2002;100:4609–14.

24. Hayakawa K, Formica AM, Brill-Dashoff J, et al. Early generated B1 B cells with restricted BCRs become chronic lymphocytic leukemia with continued c-Myc and low Bmf expression. J Exp Med. 2016;213:3007–24.

25. Hayakawa K, Formica AM, Colombo MJ, et al. Loss of a chromosomal region with synteny to human 13q14 occurs in mouse chronic lymphocytic leukemia that originates from early- generated B-1 B cells. Leukemia. 2016;30:1510–9.

26. Li Q, Wilkie AR, Weller M, et al. THY-1 Cell Surface Antigen (CD90) Has an Important Role in the Initial Stage of Human Cytomegalovirus Infection. PLoS Pathog. 2015;11:e1004999.

27. Bradley JE, Ramirez G, Hagood JS. Roles and regulation of Thy-1, a context-dependent modulator of cell phenotype. BioFactors. 2009;35:258–65.

28. Hoppo T, Fujii H, Hirose T, et al. Thy1-positive mesenchymal cells promote the maturation of CD49f-positive hepatic progenitor cells in the mouse fetal liver. Hepatology. 2004;39:1362–70.

29. Lazaro CA, Croager EJ, Mitchell C, et al. Establishment, characterization, and long-term maintenance of cultures of human fetal hepatocytes. Hepatology. 2003;38:1095–106.

30. Saalbach A, Wetzig T, Haustein UF, Anderegg U. Detection of human soluble Thy-1 in serum by ELISA. Fibroblasts and activated endothelial cells are a possible source of soluble Thy-1 in serum. Cell Tissue Res. 1999;298:307–15.

31. Jurisic G, Iolyeva M, Proulx ST, et al. Thymus cell antigen 1 (Thy1, CD90) is expressed by lymphatic vessels and mediates cell adhesion to lymphatic endothelium. Exp Cell Res. 2010;316:2982–92.

32. Kollias G, Evans DJ, Ritter M, et al. Ectopic expression of Thy-1 in the kidneys of transgenic mice induces functional and proliferative abnormalities. Cell. 1987;52:21–31.

33. Wetzel A, Chavakis T, Preissner KT, et al. Human Thy-1 (CD90) on activated endothelial cells is a counterreceptor for the leukocyte integrin Mac-1 (CD11b/CD18). J Immunol. 2004;172:3850–9.

34. Schubert K, Gutknecht D, Koberle M, et al. Melanoma cells use Thy-1 (CD90) on endothelial cells for metastasis formation. Am J Pathol. 2013;182:266–76.

35. Nosten-Bertrand M, Errington ML, Murphy KP, et al. Normal spatial learning despite regional inhibition of LTP in mice lacking Thy-1. Nature. 1996;379:826–9.

36. Underwood JR, McCall A, Csar XF. Naturally-occurring anti-thymocyte autoantibody which identifies a restricted CD4+CD8+CD3-/lo/int

37. thymocyte subpopulation exhibits extensive polyspecificity. Thymus. 1996;24:61–88.

38. Lou DQ, Nicolas G, Lesbordes JC, et al. Functional differences between hepcidin 1 and 2 in transgenic mice. Blood. 2004;103:2816–21.

38. Prentice AM. Clinical Implications of New Insights into Hepcidin-Mediated Regulation of Iron Absorption and Metabolism. Ann Nutr Metab. 2017;71:40–8.

39. Mu Y, Huo J, Guan Y, et al. An improved genome assembly for Larimichthys crocea reveals hepcidin gene expansion with diversified regulation and function. Commun Biol. 2018;1:195.

40. Athira PP, Anooja VV, Anju MV, et al. A hepatic antimicrobial peptide, hepcidin from Indian major carp, Catla catla: molecular identification and functional characterization. J Genet Eng Biotechnol. 2022;20:49.

41. Nemeth E, Ganz T. The role of hepcidin in iron metabolism. Acta Haematol. 2009;122:78–86.

42. Mu Q, Chen L, Gao X, et al. The role of iron homeostasis in remodeling immune function and regulating inflammatory disease. Sci Bull (Beijing). 2021;66:1806–16.

43. Hayakawa K, Li YS, Shinton SA, et al. Crucial Role of Increased Arid3a at the Pre-B and Immature B Cell Stages for B1a Cell Generation. Front Immunol. 2019;10:457.

44. Baumgarth N. The double life of a B-1 cell: self-reactivity selects for protective effector functions. Nat Rev Immunol. 2011;11:34–46.

45. Gross AJ, Lyandres JR, Panigrahi AK, et al. Developmental acquisition of the Lyn-CD22- SHP-1 inhibitory pathway promotes B cell tolerance. J Immunol. 2009;182:5382–92.

46. Ding C, Ma Y, Chen X, et al. Integrin CD11b negatively regulates BCR signalling to maintain autoreactive B cell tolerance. Nat Commun. 2013;4:2813.

47. Goldman N, Valiuskyte K, Londregan J, et al. Macrophage regulation of B cell proliferation. Cell Immunol. 2017;314:54–62.

48. Jacobson AC, Roundy KM, Weis JJ, Weis JH. Regulation of murine splenic B cell CR3 expression by complement component 3. J Immunol. 2009;183:3963–70.

49. Cartron G, Linassier C, Bremond JL, et al. CD5 negative B-cell chronic lymphocytic leukemia: clinical and biological features of 42 cases. Leuk Lymphoma. 1998;31:209–16.

50. Demir C, Kara E, Ekinci O, Ebinc S. Clinical and Laboratory Features of CD5-Negative Chronic Lymphocytic Leukemia. Med Sci Monit. 2017;23:2137–42.

51. Newman RA, Peterson B, Davey FR, et al. Phenotypic markers and BCL-1 gene rearrangements in B-cell chronic lymphocytic leukemia: a Cancer and Leukemia Group B study. Blood. 1993;82:1239–46.

52. Dong Q, Xiu Y, Bossler A, et al. CLL dedifferentiation to clonally related myeloid cells. Blood Adv. 2020;4:6169–74.

53. Ito S, Fujiwara SI, Mashima K, et al. Development of acute myeloid leukemia in patients with untreated chronic lymphocytic leukemia. Ann Hematol. 2017;96:719–24.

54. Ichikawa D, Asano M, Shinton SA, et al. Natural anti-intestinal goblet cell autoantibody production from marginal zone B cells. J Immunol. 2015;194:606–14.

55. Wen L, Brill-Dashoff J, Shinton SA, et al. Evidence of marginal-zone B cell-positive selection in spleen. Immunity. 2005;23:297–308.

56. Sow FB, Florence WC, Satoskar AR, et al. Expression and localization of hepcidin in macrophages: a role in host defense against tuberculosis. J Leukoc Biol. 2007;82:934–45.

57. Rosenwald A, Alizadeh AA, Widhopf G, et al. Relation of gene expression phenotype to immunoglobulin mutation genotype in B cell chronic lymphocytic leukemia. J Exp Med. 2001;194:1639–47.

58. Fais F, Ghiotto F, Hashimoto S, et al. Chronic lymphocytic leukemia B cells express restricted sets of mutated and unmutated antigen receptors. J Clin Invest. 1998;102:1515–25.

59. Prabakaran P, Chen W, Singarayan MG, et al. Expressed antibody repertoires in human cord blood cells: 454 sequencing and IMGT/HighV-QUEST analysis of germline gene usage junctional diversity, and somatic mutations. Immunogenetics. 2012;64:337–50.

60. Hong B, Wu Y, Li W, et al. In-Depth Analysis of Human Neonatal and Adult IgM Antibody Repertoires. Front Immunol. 2018;9:128.

61. Alam SM, McAdams M, Boren D, et al. The role of antibody polyspecificity and lipid reactivity in binding of broadly neutralizing anti-HIV-1 envelope human monoclonal antibodies 2F5 and 4E10 to

Hayakawa *et al. Immunity & Ageing*   (2024) 21:22

Page 22 of 24

glycoprotein 41 membrane proximal envelope epitopes. J Immunol. 2007;178:4424–35.

62. Kim YJ, Kim NY, Lee MK, et al. Overexpression and unique rearrangement of VH2 transcripts in immunoglobulin variable heavy chain genes in ankylosing spondylitis patients. Exp Mol Med. 2010;42:319–26.

63. Oakley H, Cole SL, Logan S, et al. Intraneuronal beta-amyloid aggregates, neurodegeneration, and neuron loss in transgenic mice with five familial Alzheimer's disease mutations: potential factors in amyloid plaque formation. J Neurosci. 2006;26:10129–40.

64. Robert R, Streltsov VA, Newman J, et al. Germline humanization of a murine Abeta antibody and crystal structure of the humanized recombinant Fab fragment. Protein Sci. 2010;19:299–308.

65. Robert R, Dolezal O, Waddington L, et al. Engineered antibody intervention strategies for Alzheimer's disease and related dementias by targeting amyloid and toxic oligomers. Protein Eng Des Sel. 2009;22:199–208.

66. Walter MA, Gibson WT, Ebers GC, Cox DW. Susceptibility to multiple sclerosis is associated with the proximal immunoglobulin heavy chain variable region. J Clin Invest. 1991;87:1266–73.

67. Yang Y, Li X, Ma Z, et al. CTLA-4 expression by B-1a B cells is essential for immune tolerance. Nat Commun. 2021;12:525.

68. Hayakawa K, Formica AM, Zhou Y, et al. NLR Nod1 signaling promotes survival of BCR- engaged mature B cells through up-regulated Nod1 as a positive outcome. J Exp Med. 2017;214:3067–83.

69. Hitoshi Y, Yamaguchi N, Mita S, et al. Distribution of IL-5 receptor-positive B cells. Expression of IL-5 receptor on Ly-1(CD5)+ B cells. J Immunol. 1990;144:4218–25.

70. Ponader S, Chen SS, Buggy JJ, et al. The Bruton tyrosine kinase inhibitor PCI-32765 thwarts chronic lymphocytic leukemia cell survival and tissue homing in vitro and in vivo. Blood. 2012;119:1182–9.

71. Yang R, Avery DT, Jackson KJL, et al. Human T-bet governs the generation of a distinct subset of CD11c(high)CD21(low) B cells. Sci Immunol. 2022;7:eabq3277.

72. Rubtsova K, Rubtsov AV, Cancro MP, Marrack P. Age-Associated B Cells: A T-bet- Dependent Effector with Roles in Protective and Pathogenic Immunity. J Immunol. 2015;195:1933–7.

73. Decker T, Schneller F, Hipp S, et al. Cell cycle progression of chronic lymphocytic leukemia cells is controlled by cyclin D2, cyclin D3, cyclin-dependent kinase (cdk) 4 and the cdk inhibitor p27. Leukemia. 2002;16:327–34.

74. Zhang S, Ramsay ES, Mock BA. Cdkn2a, the cyclin-dependent kinase inhibitor encoding p16INK4a and p19ARF, is a candidate for the plasmacytoma susceptibility locus, Pctr1. Proc Natl Acad Sci U S A. 1998;95:2429–34.

75. Fang MZ, Lee MH, Lee YS, et al. Low expression of cyclin D2 in G2/M-arrested and transformed proliferating Balb/3T3 cells. J Vet Med Sci. 2002;64:201–5.

76. Randazzo D, Khalique U, Belanto JJ, et al. Persistent upregulation of the beta-tubulin tubb6, linked to muscle regeneration, is a source of microtubule disorganization in dystrophic muscle. Hum Mol Genet. 2019;28:1117–35.

77. Breuss M, Heng JI, Poirier K, et al. Mutations in the beta-tubulin gene TUBB5 cause microcephaly with structural brain abnormalities. Cell Rep. 2012;2:1554–62.

78. Griffen TL, Dammer EB, Dill CD, et al. Multivariate transcriptome analysis identifies networks and key drivers of chronic lymphocytic leukemia relapse risk and patient survival. BMC Med Genomics. 2021;14:171.

79. Herman SE, Niemann CU, Farooqui M, et al. Ibrutinib-induced lymphocytosis in patients with chronic lymphocytic leukemia: correlative analyses from a phase II study. Leukemia. 2014;28:2188–96.

80. Mallm JP, Iskar M, Ishaque N, et al. Linking aberrant chromatin features in chronic lymphocytic leukemia to transcription factor networks. Mol Syst Biol. 2019;15:e8339.

81. Lu D, Zhao Y, Tawatao R, et al. Activation of the Wnt signaling pathway in chronic lymphocytic leukemia. Proc Natl Acad Sci U S A. 2004;101:3118–23.

82. Janovska P, Bryja V. Wnt signalling pathways in chronic lymphocytic leukaemia and B-cell lymphomas. Br J Pharmacol. 2017;174:4701–15.

83. Hasan MK, Ghia EM, Rassenti LZ, et al. Wnt5a enhances proliferation of chronic lymphocytic leukemia and ERK1/2 phosphorylation via a ROR1/DOCK2-dependent mechanism. Leukemia. 2021;35:1621–30.

84. Raaz U, Schellinger IN, Chernogubova E, et al. Transcription Factor Runx2 Promotes Aortic Fibrosis and Stiffness in Type 2 Diabetes Mellitus. Circ Res. 2015;117:513–24.

85. Bhatt D, Ghosh S. Regulation of the NF-kappaB-Mediated Transcription of Inflammatory Genes. Front Immunol. 2014;5:71.

86. Liu W, Chen G, Sun L, et al. TUFT1 Promotes Triple Negative Breast Cancer Metastasis, Stemness, and Chemoresistance by Up-Regulating the Rac1/beta-Catenin Pathway. Front Oncol. 2019;9:617.

87. Dou C, Zhou Z, Xu Q, et al. Hypoxia-induced TUFT1 promotes the growth and metastasis of hepatocellular carcinoma by activating the Ca(2+)/PI3K/AKT pathway. Oncogene. 2019;38:1239–55.

88. Grossmann AH, Yoo JH, Clancy J, et al. The small GTPase ARF6 stimulates beta-catenin transcriptional activity during WNT5A-mediated melanoma invasion and metastasis. Sci Signal. 2013;6:ra14.

89. Suthon S, Perkins RS, Bryja V, et al. WNT5B in Physiology and Disease. Front Cell Dev Biol. 2021;9:667581.

90. Oliver AM, Martin F, Kearney JF. Mouse CD38 is down-regulated on germinal center B cells and mature plasma cells. J Immunol. 1997;158:1108–15.

91. Damle RN, Wasil T, Fais F, et al. Ig V gene mutation status and CD38 expression as novel prognostic indicators in chronic lymphocytic leukemia. Blood. 1999;94:1840–7.

92. Zhang S, Wu CC, Fecteau JF, et al. Targeting chronic lymphocytic leukemia cells with a humanized monoclonal antibody specific for CD44. Proc Natl Acad Sci U S A. 2013;110:6127–32.

93. Sorigue M, Junca J, Sarrate E, Grau J. Expression of CD43 in chronic lymphoproliferative leukemias. Cytometry B Clin Cytom. 2018;94:136–42.

94. Nichols EM, Jones R, Watson R, et al. A CD21 low phenotype, with no evidence of autoantibodies to complement proteins, is consistent with a poor prognosis in CLL. Oncotarget. 2015;6:32669–80.

95. Kriston C, Bodor C, Szenthe K, et al. Low CD23 expression correlates with high CD38 expression and the presence of trisomy 12 in CLL. Hematol Oncol. 2017;35:58–63.

96. Christian SL. CD24 as a Potential Therapeutic Target in Patients with B-Cell Leukemia and Lymphoma: Current Insights. Onco Targets Ther. 2022;15:1391–402.

97. McWilliams L, Su KY, Liang X, et al. The human fetal lymphocyte lineage: identification by CD27 and LIN28B expression in B cell progenitors. J Leukoc Biol. 2013;94:991–1001.

98. Ranheim EA, Cantwell MJ, Kipps TJ. Expression of CD27 and its ligand, CD70, on chronic lymphocytic leukemia B cells. Blood. 1995;85:3556–65.

99. Seifert M, Sellmann L, Bloehdorn J, et al. Cellular origin and pathophysiology of chronic lymphocytic leukemia. J Exp Med. 2012;209:2183–98.

100. Kunnumbrath A, Singh N, Gupta AK, et al. Flow Cytometric Expression of CD49d in Newly Diagnosed Chronic Lymphocytic Leukemia and Its Correlation with Established Prognostic Markers. J Lab Physicians. 2022;14:435–42.

101. Hernandez C, Huebener P, Schwabe RF. Damage-associated molecular patterns in cancer: a double-edged sword. Oncogene. 2016;35:5931–41.

102. Andersson U, Tracey KJ. HMGB1 is a therapeutic target for sterile inflammation and infection. Annu Rev Immunol. 2011;29:139–62.

103. Jia L, Clear A, Liu FT, et al. Extracellular HMGB1 promotes differentiation of nurse-like cells in chronic lymphocytic leukemia. Blood. 2014;123:1709–19.

104. Ganghammer S, Gutjahr J, Hutterer E, et al. Combined CXCR3/CXCR4 measurements are of high prognostic value in chronic lymphocytic leukemia due to negative co-operativity of the receptors. Haematologica. 2016;101:e99-102.

105. Mortier A, Gouwy M, Van Damme J, et al. CD26/dipeptidylpeptidase IV-chemokine interactions: double-edged regulation of inflammation and tumor biology. J Leukoc Biol. 2016;99:955–69.

106. Bauvois B, De Meester I, Dumont J, et al. Constitutive expression of CD26/dipeptidylpeptidase IV on peripheral blood B lymphocytes of patients with B chronic lymphocytic leukaemia. Br J Cancer. 1999;79:7–8.

107. Molica S, Digiesi G, Mirabelli R, et al. Serum level of CD26 predicts time to first treatment in early B-chronic lymphocytic leukemia. Eur J Haematol. 2009;83:208–14.

Hayakawa *et al. Immunity & Ageing*   (2024) 21:22

Page 23 of 24

108. Cantaert T, Schickel JN, Bannock JM, et al. Activation-Induced Cytidine Deaminase Expression in Human B Cell Precursors Is Essential for Central B Cell Tolerance. Immunity. 2015;43:884–95.

109. Meyers G, Ng YS, Bannock JM, et al. Activation-induced cytidine deaminase (AID) is required for B-cell tolerance in humans. Proc Natl Acad Sci U S A. 2011;108:11554–9.

110. Oppezzo P, Navarrete M, Chiorazzi N. AID in Chronic Lymphocytic Leukemia: Induction and Action During Disease Progression. Front Oncol. 2021;11:634383.

111. You M, Dong G, Li F, et al. Ligation of CD180 inhibits IFN-alpha signaling in a Lyn-PI3K- BTK-dependent manner in B cells. Cell Mol Immunol. 2017;14:192–202.

112. Porakishvili N, Kulikova N, Jewell AP, et al. Differential expression of CD 180 and IgM by B-cell chronic lymphocytic leukaemia cells using mutated and unmutated immunoglobulin VH genes. Br J Haematol. 2005;131:313–9.

113. Miyazaki T, Miyazaki S, Ashida M, et al. Functional analysis of Tcl1 using Tcl1-deficient mouse embryonic stem cells. PLoS ONE. 2013;8:e71645.

114. Hinz N, Jucker M. Distinct functions of AKT isoforms in breast cancer: a comprehensive review. Cell Commun Signal. 2019;17:154.

115. Fulci V, Chiaretti S, Goldoni M, et al. Quantitative technologies establish a novel microRNA profile of chronic lymphocytic leukemia. Blood. 2007;109:4944–51.

116. Pekarsky Y, Croce CM. Is miR-29 an oncogene or tumor suppressor in CLL? Oncotarget. 2010;1:224–7.

117. Pekarsky Y, Balatti V, Croce CM. BCL2 and miR-15/16: from gene discovery to treatment. Cell Death Differ. 2018;25:21–6.

118. Robbins BA, Ellison DJ, Spinosa JC, et al. Diagnostic application of two-color flow cytometry in 161 cases of hairy cell leukemia. Blood. 1993;82:1277–87.

119. Ilyin G, Courselaud B, Troadec MB, et al. Comparative analysis of mouse hepcidin 1 and 2 genes: evidence for different patterns of expression and co-inducibility during iron overload. FEBS Lett. 2003;542:22–6.

120. Neves JV, Barroso C, Carvalho P, et al. Characterization of Erythroferrone in a Teleost Fish (Dicentrarchus labrax) With Two Functional Hepcidin Types: More Than an Erythroid Regulator. Front Immunol. 2022;13:867630.

121. Huang H, Lamikanra AA, Alkaitis MS, et al. Interleukin-10 regulates hepcidin in Plasmodium falciparum malaria. PLoS ONE. 2014;9:e88408.

122. Smith CL, Arvedson TL, Cooke KS, et al. IL-22 regulates iron availability in vivo through the induction of hepcidin. J Immunol. 2013;191:1845–55.

123. Zhang X, Deriaud E, Jiao X, et al. Type I interferons protect neonates from acute inflammation through interleukin 10-producing B cells. J Exp Med. 2007;204:1107–18.

124. Chiesa C, Pacifico L, Natale F, et al. Fetal and early neonatal interleukin-6 response. Cytokine. 2015;76:1–12.

125. Bao S, Husband AJ, Beagley KW. B1 B cell numbers and antibodies against phosphorylcholine and LPS are increased in IL-6 gene knockout mice. Cell Immunol. 1999;198:139–42.

126. Masuda K, Ripley B, Nishimura R, et al. Arid5a controls IL-6 mRNA stability, which contributes to elevation of IL-6 level in vivo. Proc Natl Acad Sci U S A. 2013;110:9409–14.

127. Diehl S, Rincon M. The two faces of IL-6 on Th1/Th2 differentiation. Mol Immunol. 2002;39:531–6.

128. Park CH, Valore EV, Waring AJ, Ganz T. Hepcidin, a urinary antimicrobial peptide synthesized in the liver. J Biol Chem. 2001;276:7806–10.

129. Nicolas G, Bennoun M, Devaux I, et al. Lack of hepcidin gene expression and severe tissue iron overload in upstream stimulatory factor 2 (USF2) knockout mice. Proc Natl Acad Sci U S A. 2001;98:8780.

130. Shaw MH, Kamada N, Kim YG, Nunez G. Microbiota-induced IL-1beta, but not IL-6, is critical for the development of steady-state TH17 cells in the intestine. J Exp Med. 2012;209:251–8.

131. Klose CS, Artis D. Innate lymphoid cells as regulators of immunity, inflammation and tissue homeostasis. Nat Immunol. 2016;17:765–74.

132. Hu L, Wu C. In silico analysis suggests disruption of interactions between HAMP from hepatocytes and SLC40A1 from macrophages in hepatocellular carcinoma. BMC Med Genomics. 2021;14:128.

133. Cheng J, Torkamani A, Grover RK, et al. Ectopic B-cell clusters that infiltrate transplanted human kidneys are clonal. Proc Natl Acad Sci U S A. 2011;108:5560–5.

134. Tian B, Yin K, Qiu X, et al. A Novel Prognostic Prediction Model Based on Pyroptosis- Related Clusters for Breast Cancer. J Pers Med. 2022;13:69.

135. Seay HR, Yusko E, Rothweiler SJ, et al. Tissue distribution and clonal diversity of the T and B cell repertoire in type 1 diabetes. JCI Insight. 2016;1:e88242.

136. Kramer KJ, Johnson NV, Shiakolas AR, et al. Potent neutralization of SARS-CoV-2 variants of concern by an antibody with an uncommon genetic signature and structural mode of spike recognition. Cell Rep. 2021;37:109784.

137. Andreano E, Paciello I, Piccini G, et al. Hybrid immunity improves B cells and antibodies against SARS-CoV-2 variants. Nature. 2021;600:530–5.

138. Zhang Y, Lee TY. Revealing the Immune Heterogeneity between Systemic Lupus Erythematosus and Rheumatoid Arthritis Based on Multi-Omics Data Analysis. Int J Mol Sci. 2022;23:5166.

139. Almqvist P, Carlsson SR. Characterization of a hydrophilic form of Thy-1 purified from human cerebrospinal fluid. J Biol Chem. 1988;263:12709–15.

140. Hammond MD, Ai Y, Sansing LH. Gr1+ Macrophages and Dendritic Cells Dominate the Inflammatory Infiltrate 12 Hours After Experimental Intracerebral Hemorrhage. Transl Stroke Res. 2012;3:s125–31.

141. Kollias G, Evans DJ, Ritter M, et al. Ectopic expression of Thy-1 in the kidneys of transgenic mice induces functional and proliferative abnormalities. Cell. 1987;51:21–31.

142. Kulaksiz H, Theilig F, Bachmann S, et al. The iron-regulatory peptide hormone hepcidin: expression and cellular localization in the mammalian kidney. J Endocrinol. 2005;184:361–70.

143. Schmidt PJ. Regulation of Iron Metabolism by Hepcidin under Conditions of Inflammation. J Biol Chem. 2015;290:18975–83.

144. Peng D, Gao Y, Zhang L, et al. The Relationship Between Hepcidin-Mediated Iron Dysmetabolism and COVID-19 Severity: A Meta-Analysis. Front Public Health. 2022;10:881412.

145. Kunireddy N, Jacob R, Khan SA, et al. Hepcidin and Ferritin: Important Mediators in Inflammation Associated Anemia in Systemic Lupus Erythematosus Patients. Indian J Clin Biochem. 2018;33:406–13.

146. Brissot P, Pietrangelo A, Adams PC, et al. Haemochromatosis. Nat Rev Dis Primers. 2018;4:18016.

147. Pratt HG, Steinberger KJ, Mihalik NE, et al. Macrophage and Neutrophil Interactions in the Pancreatic Tumor Microenvironment Drive the Pathogenesis of Pancreatic Cancer. Cancers (Basel). 2021;14:194.

148. Al-Hajj M, Wicha MS, Benito-Hernandez A, et al. Prospective identification of tumorigenic breast cancer cells. Proc Natl Acad Sci U S A. 2003;100:3983–8.

149. Tsai JH, Yang J. Epithelial-mesenchymal plasticity in carcinoma metastasis. Genes Dev. 2013;27:2192–206.

150. Peng L, Liu Z, Xiao J, et al. MicroRNA-148a suppresses epithelial-mesenchymal transition and invasion of pancreatic cancer cells by targeting Wnt10b and inhibiting the Wnt/beta- catenin signaling pathway. Oncol Rep. 2017;38:301–8.

151. Jang GY, Lee JW, Kim YS, et al. Interactions between tumor-derived proteins and Toll-like receptors. Exp Mol Med. 2020;52:1926–35.

152. Munoz DP, Lee EL, Takayama S, et al. Activation-induced cytidine deaminase (AID) is necessary for the epithelial-mesenchymal transition in mammary epithelial cells. Proc Natl Acad Sci U S A. 2013;110:E2977–86.

153. Wang C, Wang Y, Cao J, et al. Elevated expression of HMGB1 is prognostic of poor survival in patients with relapsed/refractory T/NK-CL. Ann Hematol. 2021;100:2293–302.

154. Umbreit C, Flanjak J, Weiss C, et al. Incomplete epithelial-mesenchymal transition in p16-positive squamous cell carcinoma cells correlates with beta-catenin expression. Anticancer Res. 2014;34:7061–9.

155. Geradts J, Wilson PA. High frequency of aberrant p16(INK4A) expression in human breast cancer. Am J Pathol. 1996;149:15–20.

156. Frede A, Czarnewski P, Monasterio G, et al. B cell expansion hinders the stroma-epithelium regenerative cross talk during mucosal healing. Immunity. 2022;55:2336–51.

157. Cerutti A, Cols M, Puga I. Marginal zone B cells: virtues of innate-like antibody-producing lymphocytes. Nat Rev Immunol. 2013;13:118–32.

158. Balazs M, Martin F, Zhou T, Kearney J. Blood dendritic cells interact with splenic marginal zone B cells to initiate T-independent immune responses. Immunity. 2002;17:341–52.

Hayakawa *et al. Immunity & Ageing*   (2024) 21:22

Page 24 of 24

159. Armitage AE, Stacey AR, Giannoulatou E, et al. Distinct patterns of hepcidin and iron regulation during HIV-1, HBV, and HCV infections. Proc Natl Acad Sci U S A. 2014;111:12187–92.

160. Koppensteiner H, Brack-Werner R, Schindler M. Macrophages and their relevance in Human Immunodeficiency Virus Type I infection. Retrovirology. 2012;9:82.

161. Hsieh SW, Huang LC, Chang YP, et al. M2b macrophage subset decrement as an indicator of cognitive function in Alzheimer's disease. Psychiatry Clin Neurosci. 2020;74:383–91.

162. Shevchuk SV, Zviahina OV, Kuvikova IP, Segeda IS. Level of Hepcidine in Patients with Ankylosing Spondylitis, Association with Anemia and the Severity of the Disease. Wiad Lek. 2020;73:1700.

163. Raha AA, Ghaffari SD, Henderson J, et al. Hepcidin Increases Cytokines in Alzheimer's Disease and Down's Syndrome Dementia: Implication of Impaired Iron Homeostasis in Neuroinflammation. Front Aging Neurosci. 2021;13:653591.

164. Radandish M, Khalilian P, Esmaeil N. The Role of Distinct Subsets of Macrophages in the Pathogenesis of MS and the Impact of Different Therapeutic Agents on These Populations. Front Immunol. 2021;12:667705.

165. Bsteh G, Haschka D, Tymoszuk P, et al. Serum hepcidin levels in multiple sclerosis. Mult Scler J Exp Transl Clin. 2019;5:2055217319885984.

166. Wei Y, Wang T, Liao L, et al. Brain-spleen axis in health and diseases: A review and future perspective. Brain Res Bull. 2022;182:130–40.

167. Camara-Lemarroy CR, Metz L, Meddings JB, et al. The intestinal barrier in multiple sclerosis: implications for pathophysiology and therapeutics. Brain. 2018;141:1900–16.

168. Duong L, Pixley FJ, Neison DJ, Jackaman C. Aging Leads to Increased Monocytes and Macrophages With Altered CSF-1 Receptor Expression and Earlier Tumor-Associated Macrophage Expansion in Murine Mesothelioma. Front Aging. 2022;3:848925.

169. Brookes MJ, Hughes S, Turner FE, et al. Modulation of iron transport proteins in human colorectal carcinogenesis. Gut. 2006;55:1449–60.

170. Yang Y, Wang C, Yang Q, et al. Distinct mechanisms define murine B cell lineage immunoglobulin heavy chain (IgH) repertoires. Elife. 2015;4:e09083.

171. Tian C, Luskin GK, Dischert KM, et al. Immunodominance of the VH1-46 antibody gene segment in the primary repertoire of human rotavirus-specific B cells is reduced in the memory compartment through somatic mutation of nondominant clones. J Immunol. 2008;180:3279–88.

172. Weitkamp JH, Kallewaard NL, Bowen AL, et al. VH1-46 is the dominant immunoglobulin heavy chain gene segment in rotavirus-specific memory B cells expressing the intestinal homing receptor alpha4beta7. J Immunol. 2005;174:3454–60.

173. Hong B, Wu Y, Li W, et al. In-Depth Analysis of Human Neonatal and Adult IgM Antibody Repertoires. Front Immunol. 2018;9:128.

174. Fais F, Ghiotto F, Hashimoto S, et al. Chronic lymphocytic leukemia B cells express restricted sets of mutated and unmutated antigen receptors. J Clin Invest. 1998;102:1515–25.

175. De Re V, De Vita S, Marzotto A, et al. Sequence analysis of the immunoglobulin antigen receptor of hepatitis C virus-associated non-Hodgkin lymphomas suggests that the malignant cells are derived from the rheumatoid factor-producing cells that occur mainly in type II cryoglobulinemia. Blood. 2000;96:3578–84.

176. Camacho FI, Algara P, Rodriguez A, et al. Molecular heterogeneity in MCL defined by the use of specific VH genes and the frequency of somatic mutations. Blood. 2003;101:4042–6.

177. Lindeman I, Zhou C, Eggesbo LM, et al. Longevity, clonal relationship, and transcriptional program of celiac disease-specific plasma cells. J Exp Med. 2021;218:e20200852.

178. Pennell CA, Arnold LW, Lutz PM, et al. Cross-reactive idiotypes and common antigen binding specificities expressed by a series of murine B-cell lymphomas: etiological implications. Proc Natl Acad Sci U S A. 1985;82:3799–803.

179. Chu CC, Catera R, Zhang L, et al. Many chronic lymphocytic leukemia antibodies recognize apoptotic cells with exposed nonmuscle myosin heavy chain IIA: implications for patient outcome and cell of origin. Blood. 2010;115:3907–15.

180. Forster I, Gu H, Rajewsky K. Germline antibody V regions as determinants of clonal persistence and malignant growth in the B cell compartment. EMBO J. 1988;7:3693–703.

181. Feeney AJ. Lack of N regions in fetal and neonatal mouse immunoglobulin V-D-J junctional sequences. J Exp Med. 1990;172:1377–90.

182. Conger JD, Sage HJ, Kawaguchi S, Corley RB. Properties of murine antibodies from different V region families specific for bromelain-treated mouse erythrocytes. J Immunol. 1991;146:1216–9.

183. Jiang X, Huang H, Li Z, et al. Blockade of miR-150 maturation by MLL-fusion/MYC/LIN-28 is required for MLL-associated leukemia. Cancer Cell. 2012;22:524–35.

184. Li X, Zhang J, Gao L, et al. MiR-181 mediates cell differentiation by interrupting the Lin28 and let-7 feedback circuit. Cell Death Differ. 2012;19:378–86.

185. Xiao C, Calado DP, Galler G, et al. MiR-150 controls B cell differentiation by targeting the transcription factor c-Myb. Cell. 2007;131:146–59.

186. Mraz M, Chen L, Rassenti LZ, et al. miR-150 influences B-cell receptor signaling in chronic lymphocytic leukemia by regulating expression of GAB1 and FOXP1. Blood. 2014;124:84–95.

187. Balatti V, Pekarky Y, Croce CM. Role of microRNA in chronic lymphocytic leukemia onset and progression. J Hematol Oncol. 2015;8:12.

188. Visone R, Veronese A, Rassenti LZ, et al. miR-181b is a biomarker of disease progression in chronic lymphocytic leukemia. Blood. 2011;118:3072–9.

189. Pang WW, Price EA, Sahoo D, et al. Human bone marrow hematopoietic stem cells are increased in frequency and myeloid-biased with age. Proc Natl Acad Sci U S A. 2011;108:20012–7.

190. Rumfelt LL, Zhou Y, Rowley SA, Shinton SA, Hardy RR. Lineage specification and plasticity in CD19- early B cell precursors. J Exp Med. 2006;203:675–87.

Publisher's Note